Identification of benzofused five-membered sultams, potent dual NOD1/NOD2 antagonists *in vitro* and *in vivo*

Yao Ma, Xueyuan Li, Yameng Pi, Jingjia Ye, Xiduan Wei, Jingshu Yang, Guangxu Si, Jingyuan Tian, Yi Dong, Gang Liu,

PII: S0223-5234(20)30547-X

DOI: https://doi.org/10.1016/j.ejmech.2020.112575

Reference: EJMECH 112575

To appear in: *European Journal of Medicinal Chemistry*

Received Date: 21 February 2020

Revised Date: 28 March 2020

Accepted Date: 11 June 2020

Please cite this article as: Y. Ma, X. Li, Y. Pi, J. Ye, X. Wei, J. Yang, G. Si, J. Tian, Y. Dong, G. Liu, Identification of benzofused five-membered sultams, potent dual NOD1/NOD2 antagonists *in vitro* and *in vivo*, *European Journal of Medicinal Chemistry*, https://doi.org/10.1016/j.ejmech.2020.112575.

Identification of benzofused five-membered sultams, potent dual NOD1/NOD2 antagonists *in vitro* and *in vivo*

Yao Ma [a,1], Xueyuan Li [b,1], Yameng Pi [b,1], Jingjia Ye [b], Xiduan Wei [b], Jingshu Yang [b], Guangxu Si [b], Jingyuan Tian [b], Yi Dong [a,*], Gang Liu [b,*]

[a] *Institute of Materia Medica, Chinese Academy of Medical Sciences & Peking Union Medical College, 2A Nanwei Rd, Xicheng Dist, Beijing 100050, P.R. China*

[b] *School of Pharmaceutical Sciences, Tsinghua University, Haidian Dist，Beijing 100084, P.R. China*

Abstract

Nucleotide-binding oligomerization domain-containing proteins 1 and 2 play important roles in immune system activation. Recently, a shift has occurred due to the emerging knowledge that preventing nucleotide-binding oligomerization domains (NODs) signaling could facilitate the treatment of some cancers, which warrants the search for dual antagonists of NOD1 and NOD2. Herein, we undertook the synthesis and identification of a new class of derivatives of dual NOD1/NOD2 antagonists with novel benzofused five-membered sultams. Compound **14k** was finally demonstrated to be the most potent molecule that inhibits both NOD1- and NOD2-stimulated NF-κB and MAPK signaling *in vitro* and *in vivo*.

Keywords: Five-membered sultams, Dual NOD1/NOD2 antagonist, NF-κB signaling, MAPK signaling

[1] *These authors contributed equally.*

E-mail address: dongyi@imm.ac.cn (Y. Dong), gangliu27@tsinghua.edu.cn (G. Liu)

1. Introduction

Nucleotide-binding oligomerization domain-like receptor (NLR) family proteins play a crucial role in mammalian innate immunity, serving as intracellular pattern recognition receptors (PRRs) involved in the detection of cytoplasmic pathogen-associated molecular patterns (PAMPs) and danger-associated molecular patterns (DAMPs) [1,2]. Nucleotide-binding oligomerization domain-containing proteins 1 and 2 (NOD1 and NOD2, respectively), which belong to the nodosome subgroup of NLRs, play an important role in host defense because they are the only proteins that recognize bacterial peptidoglycan components, leading to activation of NF-κB and MAPKs, resulting in an inflammatory response [3−5].

The NOD1 and NOD2 pathways have been linked to a range of inflammatory disorders [6], including inflammatory bowel disease (IBD) [7,8], Blau syndrome [9,10], rheumatoid arthritis [11,12], sarcoidosis [13], insulin resistance [14] and asthma [15−17]. Mutations and overactivation of the NOD1 and NOD2 genes have both been shown to cause immune dysregulation, which is also associated with a number of human diseases, including inflammatory disorders and cancer [5]. Recently, a shift has occurred due to the emerging knowledge that preventing NOD signaling could facilitate the treatment of some cancers [18,19]. For example, Zitvogel's group has identified the NOD2 receptor as a 'gut immune checkpoint' based on evidence that NOD2 weakens the antitumor effect of cyclophosphamide by preventing the translocation of two gut commensal species, Enterococcus hirae and Barnesiella intestinihominis, into the spleen [20]. Ferri and coworkers demonstrated NOD1 to be

a putative therapeutic target in colon cancer metastasis because NOD1 augments colon cancer metastasis *via* the p38 mitogen activated protein kinase pathway [21]. All of the above evidence warrants the urgent development of NOD1 and NOD2 antagonists.

Recently, several representative molecules based on indoline, tetrahydroisoquinoline, benzimidazole and purine scaffolds were reported to have potent NOD inhibitory activity [5]. For example, the purine-2-6-diones (**1**) [22] and benzimidazole (**2**) [23,24] were identified as active and selective NOD 1 inhibitors, while another benzimidazole (**3**) [25,26] developed at GSK was reported to selectively inhibit NOD2-mediated NF-κB signaling. Tetrahydroisoquinoline (**4**) [23] and indoline (**5**) [23,27] derivatives were found to inhibit both NOD 1 and NOD2 signaling pathways with similar inhibitory activity for NOD 1 and NOD2. We also reported that an antagonist (**7**, DY-16-43) of NOD2 signaling, conjugated muramyl dipeptide (MDP) and paclitaxel (PTX), produced sensitization to paclitaxel therapy and prevented tumor metastasis [28]. Another conjugate of an MDP derivative and docetaxel (DTX) (**8**) was also characterized as an antagonist of NOD1 signaling and was superior to DTX in breast cancer treatment [29]. Subsequently, we demonstrated that 1,4-benzodiazepine-2,5-dione (BZD) derivatives, as dual NOD1/2 antagonists (**6**), could enhance the effect of PTX in the treatment of Lewis lung carcinoma (LLC) [30]. The above evidence suggests that both NOD1 and NOD2 are indispensable for tumor survival and invasion. Effective inhibitors used for cancer treatment should antagonize both NOD1 and NOD2 signaling.

Given the potential value of NOD1/2 dual antagonists, we have developed and optimized a cell-based screening assay platform in which either NOD1 or NOD2 activation stimulates a NF-κB-responsive SEAP reporter gene as we previously described [30]. Continuously working engaged in the design, synthesis and evaluation of NOD1 and NOD2 antagonists, we found a new class of derivatives of dual NOD1/NOD2 based on a novel benzofused five-membered sultam skeleton from our compound library, which are structurally different from previously identified antagonists. Among these compounds, compound **14k** was demonstrated to be the most potent molecule that inhibited both NOD1- and NOD2- stimulated NF-κB and MAPK signaling *in vitro* and *in vivo*. The results obtained also lead to a better understanding of the structural requirements for NOD1 and NOD2 inhibition

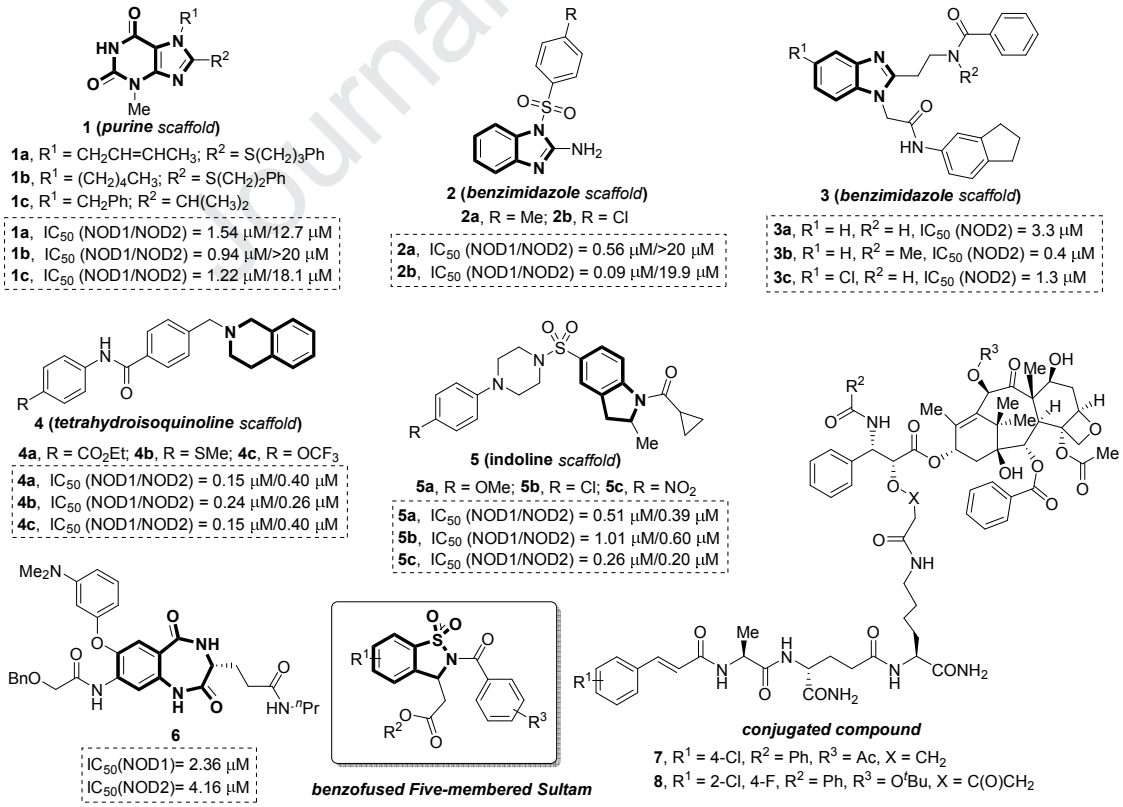

Scheme 1. Representative NOD1/2 antagonists

2. Results and discussion

2.1. Chemistry

To evaluate the antagonistic activity of NOD1/2, a series of benzofused five-membered sultams were designed and synthesized. As depicted in Scheme 2, acetylation of commercially available benzenesulfonamides (**9a-9j**) produced *N*-Ac protected analogues, which underwent Rh-catalyzed C–H alkenylation/annulation with acrylates to generate five-membered sultams (**10a-10l**) in good to excellent yields [31]. Removal of acetyl by treatment with K_2CO_3 resulted in amino-free sultam **11,** which underwent alkylation, alkenylation and acylation to yield the target compounds **12, 13** and **14**. The ^{t}-butyl ester sultam analogue (**14w**) was transformed into the corresponding acid (**15**) by treatment with trifluoroacetate, followed by amidation to produce the target amide compound **16**.

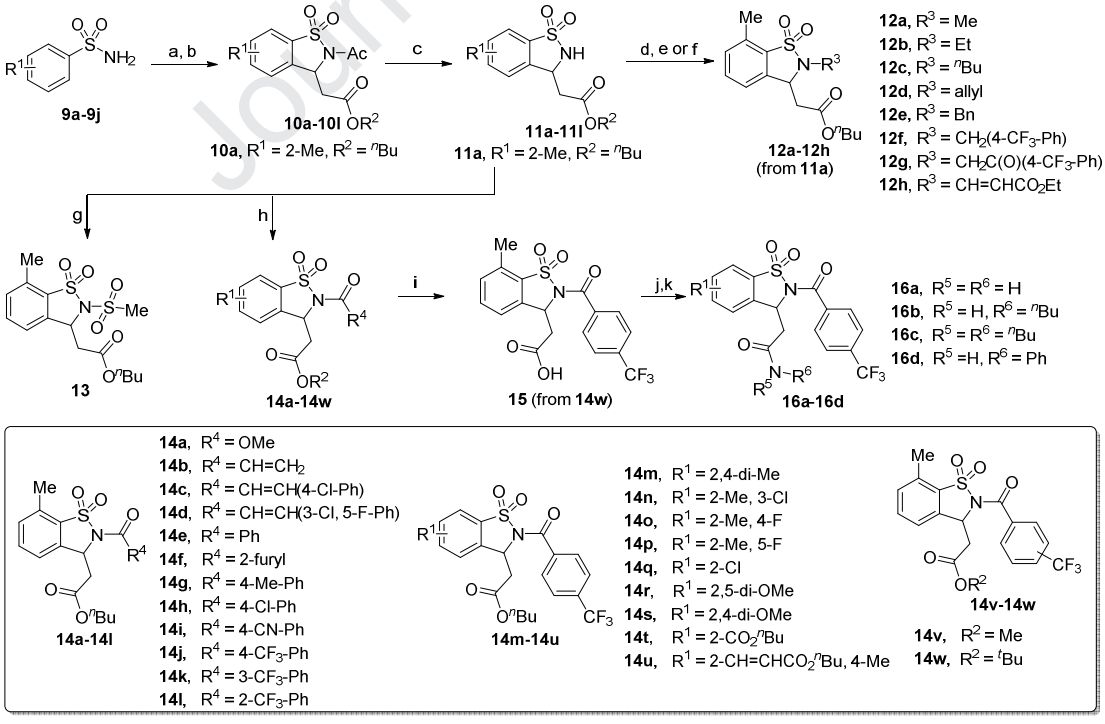

Scheme 2. General procedure for the synthesis of benzofused five-membered sultam

derivatives. Reaction conditions: (a) $ZnCl_2$, Ac_2O, rt.; (b) $[RhCp^*Cl_2]_2$, $Cu(OAc)_2$, acrylates, toluene, 100°C. (c) K_2CO_3, R^2OH, 60°C. (d) K_2CO_3, R^3X, DMF, rt. (e) R^3OH, PPh_3, DEAD, THF, rt. (f) *N*-methylmorpholine, ethyl propiolate, DCM, rt. (g) $MeSO_2Cl$, Et_3N, DCM, rt. (h) RC(O)Cl, Et_3N, DCM, rt. (i) TFA, DCM, rt. (j) $(COCl)_2$, DMF(cat.), DCM, rt. (k) R^5R^6NH, Et_3N, DCM, rt.

In presence of Cs_2CO_3 in DMF at 120°C, compound **10a** transformed into the alkene intermediate **17,** which was subsequently treated with 4-(trifluoromethyl)benzoyl chloride to afford the target compound **18**. When compound **10a** was treated with $LiAlH_4$, deacetylated alcohol intermediate **19** was obtained, followed by acylation and butylation to produce the target compound **21**.

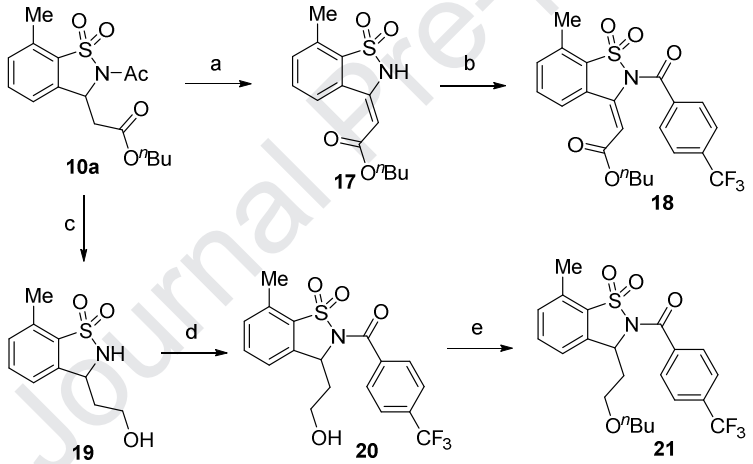

Scheme 3. Synthesis of compounds **18** and **21**. Reaction conditions: (a) Cs_2CO_3, DMF, 120°C. (b) 4-CF_3-Ph-C(O)Cl, Et_3N, DCM, rt. (c) $LiAlH_4$, THF, Ar, 0°C-rt. (d) 4-CF_3-Ph-COOH, HOSu, DIC, DMF, rt. e) 1-iodobutane, K_2CO_3, acetone, rt.

Acid intermediate **15** underwent amidation with (*E*)-*N*'-hydroxypentanimidamide to produce the intermediate **22**, followed by dehydration to yield the target 1,2,4-oxadiazole compound **23**. Additionally, the hydrazide intermediate **24** was prepared from acid intermediate **15,** followed by acylation with butyric anhydride to generate the intermediate **25,** which subsequently underwent dehydration to yield the

target 1,3,4-oxadiazole compound **26**.

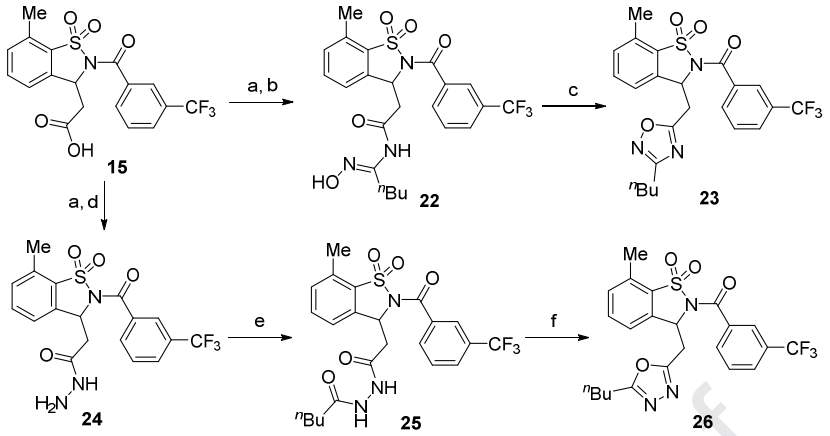

Scheme 4. Synthesis of compounds **23** and **26**. Reaction conditions: (a) $(COCl)_2$, DMF (cat.), DCM, rt. (b) (*E*)-*N*'-hydroxypentanimidamide, Et_3N, DCM, rt. (c) toluene, reflux. (d) hydrazine hydrate, Et_3N, DCM, rt. (e) butyric anhydride, Et_3N, THF, rt. (f) I_2, PPh_3, Et_3N, DCM, rt.

Sultam **11a** was treated with $DppoNH_2$ in the presence of NaH to produce sulfonyl hydrazide **27**, which further underwent acylation with 4-(trifluoromethyl)benzoyl chloride to yield the target compound **28**. 2-Methyl benzamide underwent Rh-catalyzed C–H alkenylation/annulation with butyl acrylate to yield a five-membered lactam (**29**), followed by catalytic hydrogenation and acylation to produce the target lactam compound **31**.

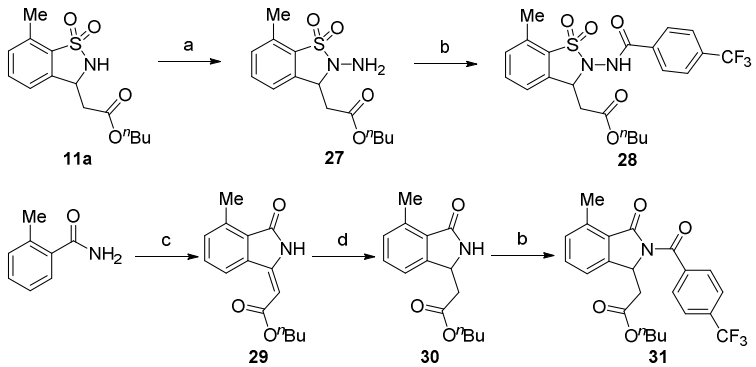

Scheme 5. Synthesis of compounds **28** and **31**. Reaction conditions: (a) NaH, $DppoNH_2$, THF, 0°C-rt. (b) 4-CF_3-Ph-C(O)Cl, Et_3N, DCM, rt. (c) $[RhCp^*Cl_2]_2$,

$AgSbF_6$, $Cu(OAc)_2$, dioxane, 120°C. (d) Pd/C, H_2, rt.

2.2. Structure-activity relationship (SAR) studies

As we previously described [30], screening for dual NOD1/2 antagonists was conducted using HEK-Blue hNOD1-secreted alkaline phosphatase (SEAP) reporter and HEK-Blue hNOD2 SEAP reporter cells activated by lauroyl-γ-D-Glu-mDAP (C12-iE-DAP) and MDP, respectively. Hit compounds were then profiled in dose-response assays and counter screened to eliminate cytotoxic compounds by the sulforhodamine B (SRB) assay.

A variety of 7-methyl benzofused five-membered sultams inserted *via* a ^{n}butyl ester chain at the C-3 position with different *N*-2 substituents were evaluated for their NOD1/2 antagonistic activity. The results clearly showed that the antagonistic activity of these sultam analogues was significantly dependent on the structure of the *N*-2 substituent (Table 1). In this SAR exploration, a series of *N*-2 substituents including hydrogen (**11a**), alkyl (**12a**-**12c**), allyl (**12d**), benzyl (**12e**), alkenyl (**12h**), acetyl (**10a**), mesyl (**13**), methoxycarbonyl (**14a**), and vinylcarbonyl (**14b**-**14d**) groups lead to low NOD1/2 inhibition rates in a single dose, while the derivatives with *N*-benzoyl groups containing Cl (**14h**), CN (**14i**) and CF_3 (**14j**) exhibited high NOD1/2 antagonistic activity with an IC_{50} of 1-5 μM. These results suggested that *N*-benzoyl is an essential group for NOD1/2 antagonistic activity and shows unique SAR dependence. When methyl-substituted benzoyl (**14e**) or furanoyl (**14f**) was attached to the nitrogen atom, no NOD1/2 antagonistic activity was observed, implying that the electron-rich aromatic membered was likely not a suitable structural unit for this activity.

Table 1. SAR of *N*-2 Substituent (R^1) Exploration [a]

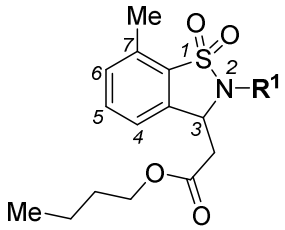

Compd.	R^1	NOD1/2 inhibition % [b]	IC_{50} (NOD1/2) μM
11a	H	-1.05±3.20/-16.81±5.22	ND/ ND
12a	Me	-25.85±1.85/4.63±5.27	ND/ ND
12b		-3.53±1.41/-1.00±3.49	ND/ ND
12c	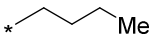	-1.50±0.60/9.07±1.49	ND/ ND
12d	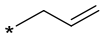	-6.10±3.26/5.52±6.62	ND/ ND
12e	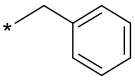	-18.12±4.34/41.38±1.44	ND/ND
12h	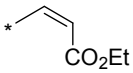	6.38±4.59/20.57±1.26	ND/ ND
10a	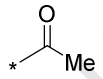	-13.86±4.51/6.59±2.55	ND/ ND
13	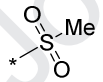	-29.24±4.45/5.29±0.97	ND/ ND
14a	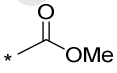	39.26±4.75/-0.67±0.98	ND/ ND
14b	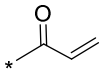	2.70±12.71/-28.20±23.55	ND/ ND
14c	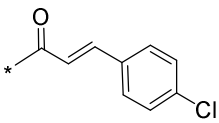	34.71±0.86/34.99±3.42	ND/ ND
14d	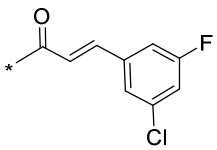	7.18±11.59/-25.07±32.49	ND/ ND
14e	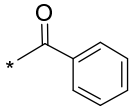	16.65±7.39/24.27±5.73	ND/ ND

14f	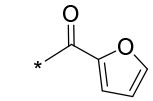	-5.44±1.21/1.83±6.79	ND/ ND
14g	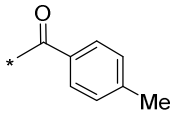	23.70±1.24/55.55±2.29	ND/ ND
14h	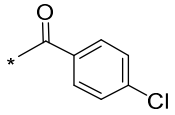	79.32±0.41/87.04±0.80	2.14±0.22/1.74±0.05
14i	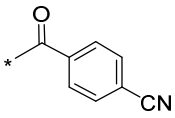	66.87±2.68/65.62±1.32	3.83±0.43/5.45±0.19
14j	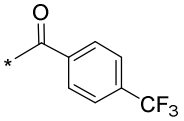	76.90±2.47/83.99±1.01	1.31±0.20/1.18±0.17

[a]All compounds were tested in C12-iE-DAP (50 ng/mL)-stimulated HEK-Blue hNOD1 cells and MDP (100 ng/mL)-stimulated HEK-Blue hNOD2 cells. ND: not determined. [b]The compounds were tested at 10 μM.

Next, we performed a detailed SAR investigation on the structural skeleton of the benzofused five-membered sultam and mainly focused on analyzing the effect of the diversity of substituents on the benzene ring with regard to the NOD1/2 antagonistic activity (Table 2). The results showed that some representative electron-donating (Me, OMe) or electron-withdrawing groups (F, Cl, ester) at different positions had little influence on the NOD1/2 antagonistic activity. However, a larger conjugated structure with an alkenyl substitution obviously lead to the loss of activity (**14u**), which implied that the benzene ring is an important and key structural unit for maintaining NOD1/2 antagonistic activity.

Table 2. SAR of R^2 Substituent Exploration [a]

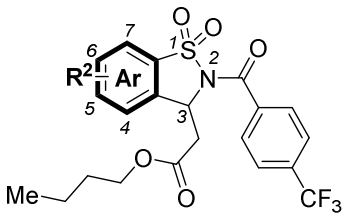

Compd.	**Ar**	NOD1/2 inhibition % [b]	IC_{50} (NOD1/2) μM
14j	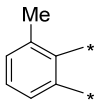	76.90±2.47/83.99±1.01	1.31±0.20/1.18±0.17
14m	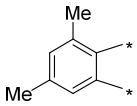	75.64±0.33/85.73±0.50	2.46±0.09/1.85±0.05
14n	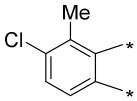	68.24±2.77/58.18±1.39	8.37±5.08/9.83±4.6
14o	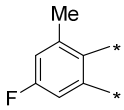	62.61±2.60/66.59±3.21	9.03±3.6/6.70±1.07
14p	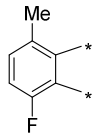	73.93±3.79/76.28±0.64	5.82±0.42/4.05±0.32
14q	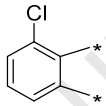	89.00±0.47/92.43±0.15	1.63±0.03/1.39±0.05
14r	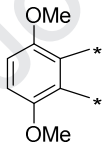	88.10±1.70/76.98±1.25	7.14±1.75/7.034±3.36
14s	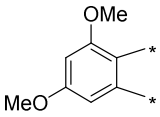	74.32±1.70/65.75±0.64	3.15±0.17/3.96±0.28
14t	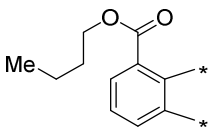	69.52±0.24/66.73±2.71	2.93±0.15/4.29±0.25
14u	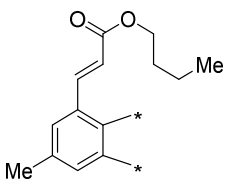	31.93±11.96/31.44±6.09	ND/ ND

[a]All compounds were tested on C12-iE-DAP (50 ng/mL)-stimulated HEK-Blue

hNOD1 cells and MDP (100 ng/mL)-stimulated HEK-Blue hNOD2 cells. ND: not determined. [b]The compounds were tested at 10 μM.

Subsequently, the C-3 substituent (R^3) was further considered, and the results are summarized in Table 3. Ester-terminated analogues exhibited high NOD1/2 antagonistic activity, including different lengths of aliphatic chain substitution (**14j**, **14v**), and sterically demanding substitution (**14w**), but the corresponding acid (**15**) and amide (**16a-16d**) analogues were likely not good NOD1/2 antagonists due to their low NOD1/2 inhibition. Removal of the carbonyl group from the ester structure resulted in the loss of activity (**21**). These results suggested that the ester group at the C-3 position plays an important role in inhibiting NOD1/2. In addition, we targeted the methylene (CH_2) attached to the C-3 position and evaluated its antagonistic effect on NOD1/2 in particular. When a C=C double bond was inserted at the C-3 position (**18**), low NOD1/2 inhibition was observed, implying that this CH_2 group, similar to the ester group attached to it, is necessary for NOD1/2 antagonistic activity.

Table 3. SAR of R^3 Substituent Exploration [a]

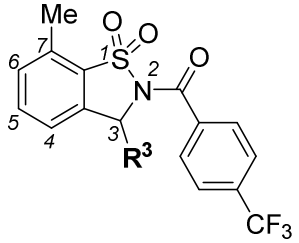

Compd.	R^3	NOD1/2 inhibition % [b]	IC_{50} (NOD1/2) μM
14j	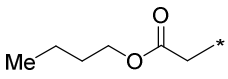	76.90±2.47/83.99±1.01	1.31±0.20/1.18±0.17
14v	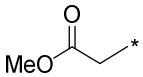	74.35±0.74/76.36±0.79	2.98±0.30/3.55±0.41
14w	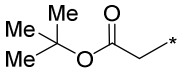	54.72±0.98/66.48±1.32	8.12±0.59/4.65±0.24

15	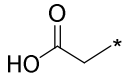	5.49±3.90/10.27±2.74	ND/ ND
16a	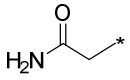	-8.79±4.30/-9.14±2.08	ND/ ND
16b	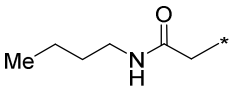	14.67±4.32/17.69±2.93	ND/ ND
16c	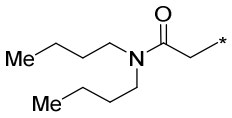	-2.01±11.43/-21.15±27.28	ND/ ND
16d	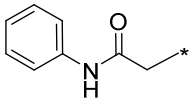	14.20±2.59/30.30±5.05	ND/ ND
18	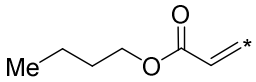	27.00±1.10/54.40±1.20	ND/ ND
21	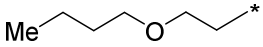	34.91±4.37/45.91±1.71	ND/ ND

[a]All compounds were tested on C12-iE-DAP (50 ng/mL)-stimulated HEK-Blue hNOD1 cells and MDP (100 ng/mL)-stimulated HEK-Blue hNOD2 cells. ND: not determined. [b]The compounds were tested at 10 μM.

To examine the necessity of the sultam skeleton and its *N*-carbonyl group, several representative compounds were evaluated (Table 4). Removal of the carbonyl group (**12f**) or addition of CH_2 (**12g**) or NH (**28**) between the carbonyl and sulfonamide groups caused a loss of NOD1/2 antagonistic activity, suggesting that the *N*-carbonyl is an essential functional group for inhibition of NOD1/2. Interestingly, the corresponding lactam analogue (**31**) was also a good NOD1/2 antagonist with an IC_{50} for NOD1/2 similar to that of the sultam analogue (**14j**).

Table 4. SAR of X and Y Substituent Exploration [a]

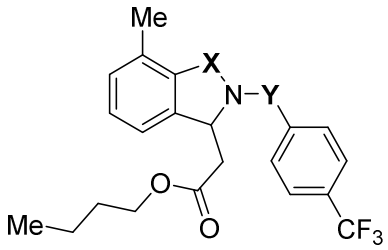

Compd.	X	Y	NOD1/2 inhibition % [b]	IC_{50} (NOD1/2) μM
14j			76.90±2.47/83.99±1.01	1.31±0.20/1.18±0.17
12f			21.69±5.72/42.54±3.41	ND/ ND
12g		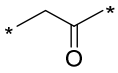	24.41±3.12/7.20±4.52	ND/ ND
28		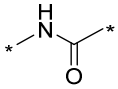	28.87±16.83/59.99±3.78	ND/ ND
31			72.02±1.11/82.73±0.74	2.47±0.19/2.36±0.29

[a]All compounds were tested on C12-iE-DAP (50 ng/mL)-stimulated HEK-Blue hNOD1 cells and MDP (100 ng/mL)-stimulated HEK-Blue hNOD2 cells. ND: not determined. [b]The compounds were tested at 10 μM.

The NOD1/2 antagonistic effect for the different substituent positions of CF_3 was examined. As shown in Table 5, *meta*-CF_3 (**14k**) or *ortho*-CF_3 (**14l**) substituted analogues showed a similar antagonistic activity, which suggested that different substituent positions of CF_3 had little effect on the antagonistic activity. The isostere of ester group was further designed and the corresponding analogues were prepared and evaluated. As shown by compounds **23** and **26**, replacement of the ester group by 1,2,4-oxadiazole or 1,3,4-oxadiazole led to NOD1/2 antagonistic activity similar to

that of ester analogue **14k**, which suggested that the ester group at the C-3 position or its isostere is a key structural unit necessary for NOD1/2 antagonistic activity.

Table 5. SAR of Z and CF_3 Substituent Exploration [a]

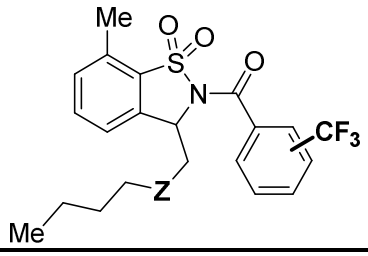

Compd.	**Z**	*o*-, *m*- or *p*-**CF_3**	NOD1/2 inhibition % [b]	IC_{50} (NOD1/2) μM
14j		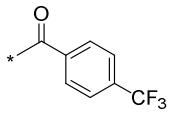	76.90±2.47/83.99±1.01	1.31±0.20/1.18±0.17
14k		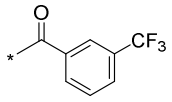	87.73±0.33/89.65±0.29	1.05±0.05/0.93±0.03
14l		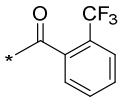	80.32±0.96/90.38±1.17	1.10±0.06/0.48±0.02
23	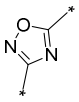	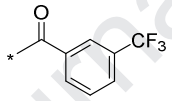	73.07±1.64/78.43±0.60	0.23±0.02/5.74±5.24
26		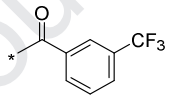	85.03±2.24/91.3±0.28	1.74±0.16/4.65±0.24

[a]All compounds were tested on C12-iE-DAP (50 ng/mL)-stimulated HEK-Blue hNOD1 cells and MDP (100 ng/mL)-stimulated HEK-Blue hNOD2 cells. ND: not determined. [b]The compounds were tested at 10 μM.

In summary, 45 compounds were synthesized and tested on C12-iE-DAP (50 ng/mL)-stimulated HEK-Blue hNOD1 cells and MDP (100 ng/mL)-stimulated HEK-Blue hNOD2 cells to evaluate their NOD1/2 antagonistic activity, and the SAR is summarized in Fig. 1. For the ***A*** structural fragment, a series of groups including H, F, Cl, Me, OMe and ester groups at different positions were well tolerated with regard

to NOD1/2 antagonistic activity, but an alkenyl substituent resulted in a low level of NOD1/2 inhibition. For the ***B*** structural fragment, a C=C double bond at the C-3 position caused a loss of activity, implying that the α, β-unsaturated side chain at the C-3 position is not beneficial for NOD1/2 antagonistic activity. Compared to the ester-terminated analogue and its isostere, the amide-terminated compounds did not exhibit obvious NOD1/2 antagonistic activity, and a free carboxyl group appeared to result in a complete loss of NOD1/2 antagonistic activity because it could prevent the compound from interacting with NOD1/2. For the ***C*** structural fragment, the corresponding lactam analogue showed similar inhibitory activity to the sultam, implying that this sultam or lactam structure unit is necessary for NOD1/2 antagonistic activity. For the ***D*** structural fragment, only the N-benzoyl group substituted by Cl, CN or CF_3 resulted in potent NOD1/2 antagonistic activity. Additionally, removal of the carbonyl or addition of CH_2 or NH resulted in a complete loss of NOD1/2 antagonistic activity, which suggests that N-benzoyl is a key structural unit for inhibition of NOD1/2. Based on the SAR described above, compound **14k** was selected as a model compound to evaluate the cytotoxicity and anti-inflammatory effects in animals.

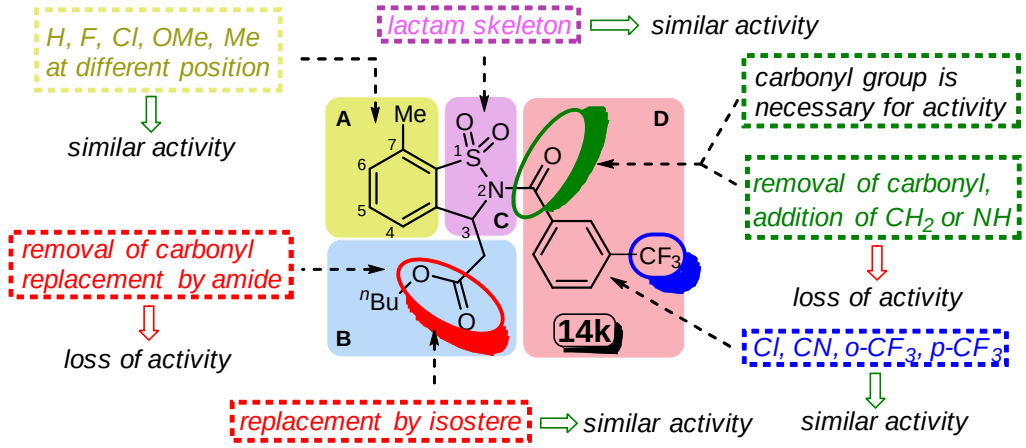

Fig. 1. SAR exploration for benzofused five-membered sultam compounds

2.3. Biological profiling

HEK-Blue hNOD1 and HEK-Blue hNOD2 cells were preincubated with different concentrations of compound **14k** for 3 h and then stimulated with C12-iE-DAP (50 ng/mL) and MDP (100 ng/mL) for an additional 20 h. SEAP was quantified as described in the Experimental Section. As shown in Fig. 2A, compound **14k** exhibited promising potent inhibitory activity against NOD1 and NOD2 with IC_{50} values of 1.05 and 0.93 μM, respectively, and no cytotoxicity (Fig. 2B).

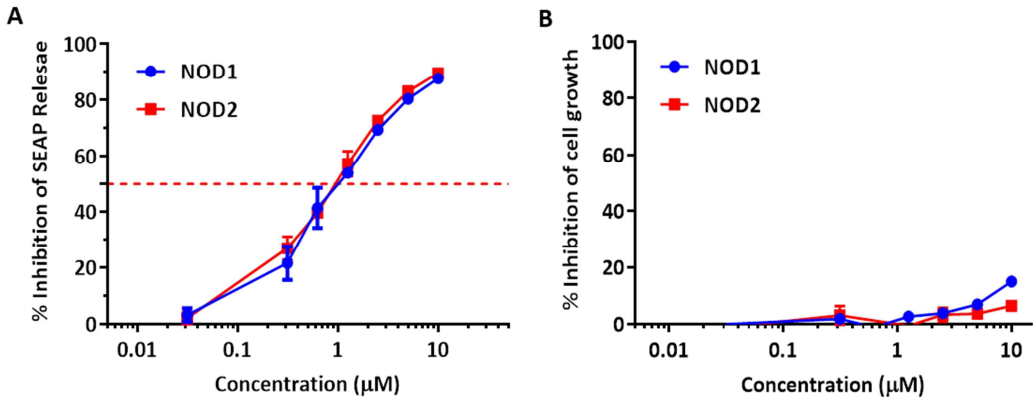

Fig. 2. (A) Compound **14k** inhibits C12-iE-DAP and MDP-induced NF-κB activation. HEK-Blue hNOD1 and HEK-Blue hNOD2 cells were preincubated with different concentrations of compound **14k** for 3 h and then stimulated with C12-iE-DAP (50 ng/mL) and MDP (100 ng/mL) for an additional 20 h. SEAP was quantified as

described in the Experimental Section. Data are presented as the mean ± standard deviation (SD) (n = 3). (B) Compound **14k** had little or no effect on cell growth. Following SEAP quantification, cells were fixed with 80% TCA at 4°C for 1 h and stained with SRB in 1% acetic acid for 10 minutes. Then, the plates were washed five times and air-dried at room temperature (rt). Bound stain was subsequently solubilized with 10 mM Tris base (150 μL), and the absorbance was measured with a spectrophotometer at 515 nm. The inhibition rate of cell growth was calculated by the following formula: [(C-T)/C] × 100 (C, OD of control group; T, OD of the compound **14k**-treated group). Data are presented as the mean ± SD (n=3).

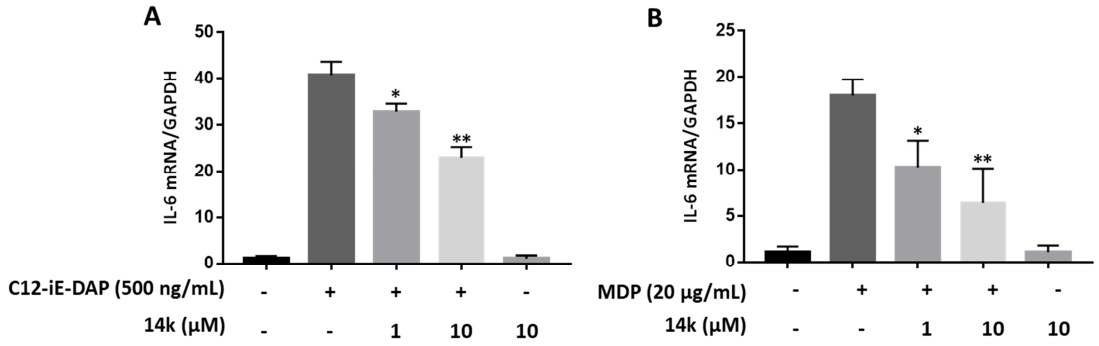

Fig. 3. Suppression of IL-6 expression in THP-1 cells by **14k**. THP-1 cells were treated with or without compound **14k** (1 μM or 10 μM) for 1 h and then stimulated with (left) C12-iE-DAP (500 ng/mL) or (right) MDP (20 μg/mL) for 90 minutes. The mRNA level of IL-6 was determined by qRT-PCR. Data are presented as the mean ± standard deviation (SD) (n =3): (∗) $p < 0.05$, (∗∗) $p < 0.01$, (∗∗∗) $p < 0.001$ vs the C12-iE-DAP- or MDP-treated group.

The activity of compound **14k** on endogenous NOD1 and NOD2 receptors was determined by inhibition of either C12-iE-DAP- or MDP-stimulated IL-6 transcription, respectively, using THP-1 human myeloid leukemia mononuclear cells. These cells have been demonstrated to express native functional NOD1 and NOD2 and respond to NOD activation with increased NF-κB activity and secretion of

inflammatory cytokines [32]. As shown in Fig. 3, pretreatment of THP-1 cells with compound **14k** consistently and dose-dependently reduced the transcription of IL-6 stimulated by C12-iE-DAP and MDP, respectively, which suggested that compound **14k** inhibits both the NOD1 and NOD2 signaling pathways in human immune cells.

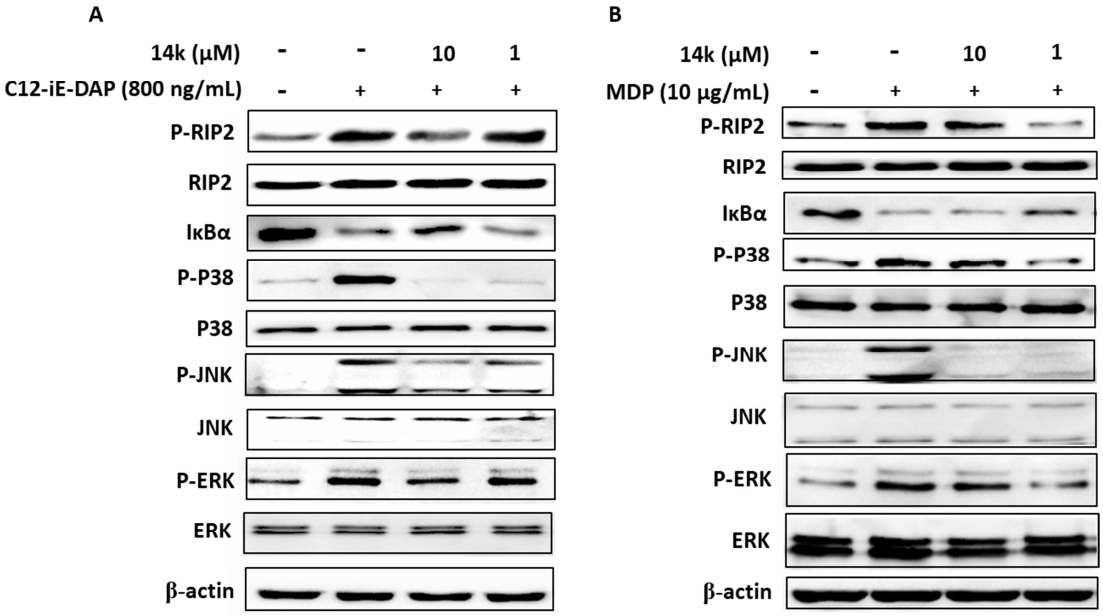

Fig. 4. Compound **14k** suppresses inflammation *via* NOD1 and NOD2 activation. Serum-starved THP1 cells were pretreated with or without compound **14k** (1 μM or 10 μM) for 1 h prior to (A) C12-iE-DAP (800 ng/mL) or (B) MDP (10 μg/mL) treatment for 30 minutes. The levels of IκBα, total and phosphorylated RIP2, JNK, p38, and ERK1/2 were determined by Western blotting. β-Actin was used as a loading control.

The activation of NOD1 and NOD2 signaling, which leads to the release of proinflammatory chemokines, is mediated by the phosphorylation of a cascade of effector proteins, including RIP2, extracellular signal-regulated kinase (ERK), p38, c-Jun N-terminal kinase (JNK), and IκBα [33]. To determine whether compound **14k**

inhibited both the NOD1 and NOD2 pathways, the effects on total IκBα and phosphorylated p38, p-JNK and p-ERK levels were tested in THP-1 cells stimulated with C12-iE-DAP or MDP, respectively. Pre-treatment of cells with compound **14k** at 1 and 10 μM prevented C12-iE-DAP-induced increases in p-RIP2, p-p38, p-JNK, and p-ERK and C12-iE-DAP-induced reduction in total IκBα in THP-1 cells. As expected, compound **14k** inhibited similar effects induced by MDP (Fig. 4B). These findings demonstrate that compound **14k** inhibits both the NF-κB and MAPK signaling pathways following activation of NOD1 and NOD2.

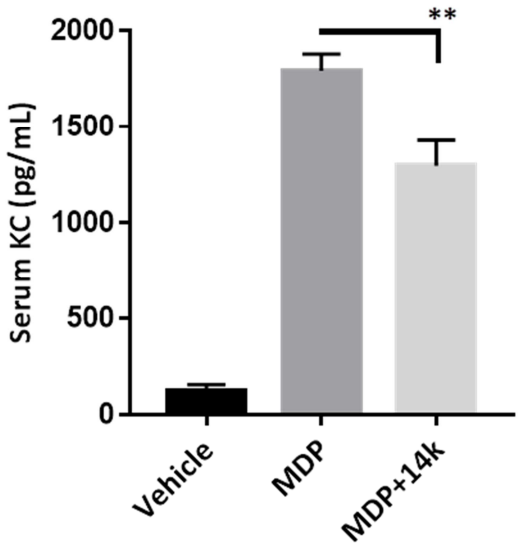

Fig. 5. Compound **14k** inhibited MDP-induced inflammatory responses *in vivo*. Intravenous injection of compound **14k** (50 mg/kg) produced moderate inhibition of serum KC in mice following an intraperitoneal challenge with MDP (4 mg/kg). Data are presented as the mean ± SEM (n =10): (∗∗) $p < 0.01$ vs MDP-treated group.

To demonstrate the utility of compound **14k** *in vivo*, we employed a model in which the systemic inflammatory response to an intraperitoneal injection of MDP or Tri-DAP was measured in mice after administration of 50 mg/kg of compound **14k**. A

single intravenous dose of 50 mg/kg of compound **14k** produced moderate inhibition of serum KC (the rodent orthologue of IL-8) in mice following intraperitoneal challenge with MDP (4 mg/kg) (Fig. 5). However, intraperitoneal injection of Tri-DAP (up to 20 mg/kg) produced only weak induction of serum KC, and a reduction of this level by compound **14k** was barley observed (data not shown). Since compound **14k** only had moderate inhibition effect on cytokine production in response to stimulation with MDP in vivo, which is less effective in mice than compound (**6**) that we previously reported. It may currently not good enough to be an ideal drug candidate used for adjuvant cancer chemotherapy. Nonetheless, our preliminary studies have indicated that these sultam derivatives had potential value for continued development. Meanwhile, given the limited structure number of the currently reported NOD1/2 antagonists, the discovery of benzofused five-membered sultam dual NOD1/NOD2 antagonist increased the scaffold diversity of NOD1/2 antagonists, and potentially provided a novel lead compound for further optimization to get more ideal NOD1/2 antagonists. Further work focused on improvement of potency and pharmacological profile of **14k** will be performed.

3. Conclusions

We report the synthesis and identification of a new class of derivatives of dual NOD1/NOD2 antagonists based on a novel benzofused five-membered sultam skeleton, which is structurally different from previously identified antagonists. Compound **14k** was demonstrated to be the most potent molecule that suppressed both NOD1- and NOD2- stimulated NF-κB and MAPK signaling *in vitro* and *in vivo*.

The results obtained also lead to a better understanding of the structural requirements for NOD1 and NOD2 inhibition and enriched the scaffold diversity of NOD1/2 antagonists. Further improvement of the potency and druggability of these compounds will be elaborated.

4. Experimental

4.1 General

Toluene, DCM, *n*-BuOH, *t*-BuOH, DMF and other commercial reagents were purchased from domestic corporations and used without further purification. Analytical thin-layer chromatography (TLC) plates, preparative TLC plates, and silica gel for column chromatography were purchased from Qingdao Haiyang Chemical and Special Silica Gel Co, Ltd. High-resolution LCMS was conducted using Agilent LC/MSD TOF with an Agilent ZORBAX SB-C18 (rapid resolution, 3.5 μm, 2.1 mm × 30 mm) column at a flow rate of 0.40 mL/min. The solvent was MeOH/water (75:25 (v/v)) containing 5 mmol/L ammonium formate. The ion source was electrospray ionization (ESI). The automatic liquid chromatography−mass spectrometry (LCMS) analysis was performed on a Waters SQ Advantage mass spectrometer equipped with an ultraperformance LC (UPLC) system and an eluent splitter (5% eluent was split into the MS system).

Proton nuclear magnetic resonance was performed on a Bruker Advance 300NMR or 400 NMR spectrometer depending on its necessary. The chemical shifts of the ^{1}H NMR spectra are reported in units of parts per million (ppm) downfield from SiMe4 (δ 0.0) and relative to the signals of chloroform-d (δ = 7.26 ppm, singlet).

Multiplicities are described as follows: s (singlet), brs (broad singlet), d (doublet), t (triplet), q (quartet), dd (doublet of doublets), and m (multiplets). The number of protons (n) for a given resonance is indicated by nH. The chemical shifts of the ^{13}C NMR spectra are reported in units of ppm downfield from SiMe4 (δ 0.0) and relative to the signals of chloroform-d (δ = 77.16 ppm, triplet).

The compounds **10a-10l**, **11a**, **12a-12e**, **12g-12h**, **13**, **14a**, **14j** were synthesized according to our previous report [31].

General synthetic procedure of compounds **12f** *and* **12g**. K_2CO_3 (2.0 equivalent, 27.6mg) and R^3X (1.5 equivalent) were added to a solution of compound **11a** (0.1 mmol, 30 mg) in 5 mL of DMF, and the reaction mixture was stirred at room temperature and monitored by LCMS until all of the starting material was consumed completely. Solvent was removed *in vacuo*, and the residue was diluted with 10 mL of ethyl acetate, washed with 10 mL water, and extracted with ethyl acetate two times. Then the organic phase was combined, washed with brine, and dried over anhydrous Na_2SO_4. The organic layer was concentrated and purified with column chromatography on silica gel to afford compounds **12f** and **12g**.

Butyl 3-(7-methyl-1,1-dioxido-2-(4-(trifluoromethyl)benzyl)-2,3-dihydrobenzo[d]isothiazol-3-yl)-2-oxopropanoate (**12f**). (36.8 mg, 81% yield). ^1H NMR (400 MHz, $CDCl_3$) δ 7.59 (q, *J* = 8.4 Hz, 4H), 7.49 (t, *J* = 7.6 Hz, 1H), 7.31 (d, *J* = 7.6 Hz, 1H), 7.16 (d, *J* = 7.7 Hz, 1H), 4.82 (t, *J* = 5.7 Hz, 1H), 4.64 (s, 2H), 4.02 – 3.87 (m, 2H), 2.83 (dd, *J* = 16.4, 6.1 Hz, 1H), 2.74 (dd, *J* = 16.4, 5.7 Hz, 1H), 2.69 (s, 3H), 1.51 – 1.42 (m, 2H),

1.24 (dq, *J* = 14.5, 7.2 Hz, 2H), 0.87 (t, *J* = 7.3 Hz, 3H). ^{13}C NMR (100 MHz, $CDCl_3$) δ 170.4, 140.4 137.4, 134.6, 133.2, 133.1, 131.2, 130.2, 128.8, 125.8 (q, *J* = 3.7 Hz), 124.2 (d, *J* = 272.0 Hz), 121.4, 65.3, 57.5, 46.8, 40.0, 30.5, 19.1, 17.1, 13.7. mp: 68−70 °C. HRMS (ESI): m/z ($M+H^+$) calcd for $C_{22}H_{25}O_4NF_3S$, 456.1451, found: 456.1451.

Butyl 3-(7-methyl-1,1-dioxido-2-(2-oxo-2-(4-(trifluoromethyl)phenyl)ethyl)-2,3-dihydrobenzo[d]isothiazol-3-yl)-2-oxopropanoate (**12g**). (36.2 mg, 75% yield). ^{1}H NMR (400 MHz, $CDCl_3$) δ 8.05 (d, *J* = 8.1 Hz, 2H), 7.75 (d, *J* = 8.1 Hz, 2H), 7.52 (t, *J* = 7.6 Hz, 1H), 7.31 (d, *J* = 7.5 Hz, 1H), 7.21 (d, *J* = 7.7 Hz, 1H), 5.15 (dd, *J* = 8.8, 3.4 Hz, 1H), 5.01 (q, *J* = 18.7 Hz, 2H), 4.06 (t, *J* = 6.7 Hz, 2H), 2.98 (dd, *J* = 17.2, 8.9 Hz, 1H), 2.86 (dd, *J* = 17.2, 3.6 Hz, 1H), 2.66 (s, 3H), 1.60 – 1.51 (m, 2H), 1.31 (dt, *J* = 15.0, 7.6 Hz, 2H), 0.90 (t, *J* = 7.4 Hz, 3H). ^{13}C NMR (100 MHz, $CDCl_3$) δ 193.9, 171.4, 138.2, 137.6, 135.1 (q, *J* = 32.7 Hz), 134.3, 133.8, 133.2, 131.0, 128.5, 126.0 (q, *J* = 3.6 Hz), 123.6 (d, *J* = 272.9 Hz), 121.3, 65.3, 58.5, 51.4, 41.5, 30.6, 19.2, 17.1, 13.8. mp: 88−90 °C. HRMS (ESI): m/z ($M+H^+$) calcd for $C_{23}H_{25}O_5NF_3S$, 484.1400; found: 484.1400.

General synthetic procedure of compound **14b-14w**. Et_3N (3.0 equivalent, 41 mg) and $R^4C(O)Cl$ (1.5 equivalent) was added to a solution of compound **11a** (0.1 mmol, 30 mg) in 1 mL of DCM, and the reaction mixture was stirred at room temperature and monitored by LCMS until all of the starting material was consumed completely. Solvent was removed *in vacuo*, and the residue was diluted with 10 mL of ethyl

acetate, washed with 10 mL water, and extracted with ethyl acetate two times. Then the organic phase was combined, washed with brine, and dried over anhydrous Na_2SO_4. The organic layer was concentrated and purified with column chromatography on silica gel to afford compounds **14b-14w**.

Butyl 3-(2-acryloyl-7-methyl-1,1-dioxido-2,3-dihydrobenzo[d]isothiazol-3-yl)-2-oxopropanoate (**14b**). (30.2 mg, 86% yield). ^{1}H NMR (400 MHz, $CDCl_3$) δ 7.56 (t, *J* = 7.7 Hz, 1H), 7.35 (dd, *J* = 12.3, 7.6 Hz, 2H), 7.08 (dd, *J* = 16.6, 10.4 Hz, 1H), 6.61 (dd, *J* = 16.6, 1.4 Hz, 1H), 5.97 (dd, *J* = 10.4, 1.4 Hz, 1H), 5.76 (dd, *J* = 7.7, 3.3 Hz, 1H), 4.07 (t, *J* = 6.7 Hz, 2H), 3.16 (dd, *J* = 16.0, 3.4 Hz, 1H), 2.95 (dd, *J* = 16.0, 7.7 Hz, 1H), 2.65 (s, 3H), 1.57 – 1.49 (m, 2H), 1.27 (dq, *J* = 14.2, 7.2 Hz, 2H), 0.88 (t, *J* = 7.4 Hz, 3H). ^{13}C NMR (100 MHz, $CDCl_3$) δ 169.8, 162.9, 135.4, 135.0, 134.3, 132.2, 132.1, 131.6, 127.9, 122.1, 65.1, 55.0, 39.3, 30.5, 19.1, 17.0, 13.8. HRMS (ESI): m/z ($M+H^+$) calcd for $C_{17}H_{22}O_5NS$, 352.1213, found: 352.1213.

Butyl (E)-3-(2-(3-(4-chlorophenyl)acryloyl)-7-methyl-1,1-dioxido-2,3-dihydrobenzo[d]isothiazol-3-yl)-2-oxopropanoate (**14c**). (34.6 mg, 75% yield). ^{1}H NMR (400 MHz, $CDCl_3$) δ 7.83 (d, *J* = 15.4 Hz, 1H), 7.56 (dd, *J* = 8.1, 6.5 Hz, 3H), 7.59 – 7.52 (m, 3H), 7.40 – 7.31 (m, 5H), 4.08 (td, *J* = 6.6, 0.9 Hz, 2H), 3.20 (dd, *J* = 16.0, 3.4 Hz, 1H), 2.99 (dd, *J* = 16.0, 7.6 Hz, 1H), 2.67 (s, 3H), 1.57 – 1.49 (m, 2H), 1.30 – 1.24 (m, 2H), 0.86 (t, *J* = 7.4 Hz, 3H). ^{13}C NMR (100 MHz, $CDCl_3$) δ 169.8, 163.0, 144.7, 136.9, 135.5, 135.0, 134.3, 132.8, 132.3, 131.6, 129.9, 129.3, 122.1, 118.1, 65.1, 55.1, 39.3, 30.5,

19.1, 17.0, 13.8. mp: 144−146 °C. HRMS (ESI): m/z ($M+H^+$) calcd for $C_{23}H_{25}O_5NClS$, 462.1136, found: 462.1138.

Butyl (E)-3-(2-(3-(3-chloro-5-fluorophenyl)acryloyl)-7-methyl-1,1-dioxido-2,3-dihydrobenzo[d]isothiazol-3-yl)-2-oxopropanoate (**14d**). (34.5 mg, 72% yield). ^{1}H NMR (400 MHz, $CDCl_3$) δ 8.22 (d, *J* = 15.4 Hz, 1H), 7.77 (dd, *J* = 8.8, 6.0 Hz, 1H), 7.57 (t, *J* = 7.7 Hz, 1H), 7.40 – 7.28 (m, 3H), 7.18 (dd, *J* = 8.4, 2.6 Hz, 1H), 7.03 (td, *J* = 8.2, 2.5 Hz, 1H), 5.81 (dd, *J* = 7.6, 3.3 Hz, 1H), 4.08 (t, *J* = 6.7 Hz, 2H), 3.21 (dd, *J* = 16.0, 3.4 Hz, 1H), 3.00 (dd, *J* = 16.0, 7.6 Hz, 1H), 2.66 (s, 3H), 1.57 – 1.49 (m, 2H), 1.27 (dq, *J* = 14.9, 7.4 Hz, 2H), 0.87 (t, *J* = 7.4 Hz, 3H). ^{13}C NMR (100 MHz, $CDCl_3$) δ 169.8, 162.6, 163.7 (d, *J* = 253.1 Hz), 140.7, 136.6 (d, *J* = 10.4 Hz), 135.5, 135.0, 134.3, 132.2, 131.6, 129.7 (d, *J* = 9.2 Hz), 129.0 (d, *J* = 3.7 Hz), 122.1, 119.7 (d, *J* = 2.1 Hz), 117.6 (d, *J* = 24.8 Hz), 115.0 (d, *J* = 21.7 Hz), 65.1, 55.2, 39.3, 30.6, 19.1, 17.0, 13.7. mp: 92−94 °C. HRMS (ESI): m/z ($M+H^+$) calcd for $C_{23}H_{24}O_5NClFS$, 480.1042, found: 480.1050.

Butyl 3-(2-benzoyl-7-methyl-1,1-dioxido-2,3-dihydrobenzo[d]isothiazol-3-yl)-2-oxopropanoate (**14e**). (37.3 mg, 93% yield). ^{1}H NMR (400 MHz, $CDCl_3$) δ 7.90 (d, *J* = 7.5 Hz, 2H), 7.65 – 7.46 (m, 4H), 7.39 (d, *J* = 7.8 Hz, 1H), 7.31 (d, *J* = 7.5 Hz, 1H), 6.14 (t, *J* = 5.7 Hz, 1H), 4.09 (t, *J* = 6.7 Hz, 2H), 3.14 – 2.99 (m, 2H), 2.55 (s, 3H), 1.58 – 1.44 (m, 2H), 1.26 (dq, *J* = 14.9, 7.2 Hz, 2H), 0.86 (t, *J* = 7.4 Hz, 3H). ^{13}C NMR (100 MHz, $CDCl_3$) δ 169.6, 168.5, 135.4, 134.9, 134.6, 134.1, 132.8, 131.6, 128.7, 128.5, 122.1,

65.2, 54.9, 40.1, 30.5, 19.1, 16.9, 13.7. mp: 59−61 °C. HRMS (ESI): m/z ($M+H^+$) calcd for $C_{21}H_{24}O_5NS$, 402.1370, found: 402.1373.

Butyl 3-(2-(furan-2-carbonyl)-7-methyl-1,1-dioxido-2,3-dihydrobenzo[d]isothiazol-3-yl)-2-oxopropanoate (**14f**). (34.8 mg, 89% yield). ^{1}H NMR (400 MHz, $CDCl_3$) δ 7.72 (s, 1H), 7.66 (s, 1H), 7.57 (t, *J* = 7.6 Hz, 1H), 7.43 – 7.31 (m, 2H), 6.61 (s, 1H), 6.18 (t, *J* = 4.7 Hz, 1H), 4.07 (t, *J* = 6.0 Hz, 2H), 3.08 – 2.94 (m, 2H), 2.64 (s, 3H), 1.55 – 1.46 (m, 2H), 1.30 – 1.19 (m, 2H), 0.86 (t, *J* = 7.3 Hz, 3H). ^{13}C NMR (100 MHz, $CDCl_3$) δ 169.6, 156.2, 147.3, 146.0, 135.4, 134.9, 134.1, 132.8, 131.7, 120.0, 120.3, 112.4, 65.2, 54.8, 40.2, 30.5, 19.1, 17.0, 13.8. mp: 180−182 °C.

Butyl 2-(7-methyl-2-(4-methylbenzoyl)-1,1-dioxido-2,3-dihydrobenzo[d]isothiazol-3-yl)acetate (**14g**). (39.4 mg, 95% yield). ^{1}H NMR (400 MHz, $CDCl_3$) δ 7.82 (d, *J* = 8.0 Hz, 2H), 7.56 (t, *J* = 7.7 Hz, 1H), 7.38 (d, *J* = 7.8 Hz, 1H), 7.31 (d, *J* = 7.7 Hz, 3H), 6.15 (t, *J* = 5.6 Hz, 1H), 4.08 (t, *J* = 6.6 Hz, 2H), 3.11 – 2.99 (m, 2H), 2.55 (s, 3H), 2.43 (s, 3H), 1.57 – 1.47 (m, 2H), 1.26 (dq, *J* = 15.0, 7.3 Hz, 2H), 0.86 (t, *J* = 7.3 Hz, 3H). ^{13}C NMR (100 MHz, $CDCl_3$) δ 169.6, 168.5, 143.6, 135.4, 134.8, 134.0, 131.8, 131.5, 129.2, 128.8, 122.0, 65.2, 54.8, 40.1, 30.5, 21.9, 19.1, 16.9, 13.7. mp: 89−90 °C. HRMS (ESI): m/z ($M+H^+$) calcd for C22 H26 O5 N S, 416.1526, found: 416.1528.

Butyl 2-(2-(4-chlorobenzoyl)-7-methyl-1,1-dioxido-2,3-dihydrobenzo[d]isothiazol-3-yl)acetate (**14h**). (39.6 mg, 91% yield). ^{1}H NMR (400 MHz, $CDCl_3$) δ 7.85 (d, *J* = 8.3 Hz,

2H), 7.57 (t, *J* = 7.7 Hz, 1H), 7.48 (d, *J* = 8.2 Hz, 2H), 7.38 (d, *J* = 7.8 Hz, 1H), 7.32 (d, *J* = 7.5 Hz, 1H), 6.12 (t, *J* = 5.7 Hz, 1H), 4.07 (t, *J* = 6.7 Hz, 2H), 3.05 (d, *J* = 5.7 Hz, 2H), 2.55 (s, 3H), 1.56 – 1.45 (m, 2H), 1.25 (dq, *J* = 14.6, 7.4 Hz, 3H), 0.86 (t, *J* = 7.3 Hz, 3H). ^{13}C NMR (100 MHz, $CDCl_3$) δ 169.5, 167.5, 139.3, 135.2, 134.9, 134.2, 132.9, 132.6, 131.6, 130.2, 128.9, 122.1, 65.3, 54.9, 40.0, 30.5, 19.1, 16.9, 13.7. mp: 62−64 °C. HRMS (ESI): m/z ($M+H^+$) calcd for $C_{21}H_{23}O_5NClS$, 436.0980, found: 436.0977.

Butyl 2-(2-(4-cyanobenzoyl)-7-methyl-1,1-dioxido-2,3-dihydrobenzo[d]isothiazol-3-yl)acetate (**14i**). (37.9 mg, 89% yield). ^{1}H NMR (400 MHz, $CDCl_3$) δ 7.96 (d, *J* = 8.1 Hz, 2H), 7.79 (d, *J* = 8.0 Hz, 2H), 7.59 (t, *J* = 7.7 Hz, 1H), 7.40 (d, *J* = 7.8 Hz, 1H), 7.34 (d, *J* = 7.5 Hz, 1H), 6.08 (t, *J* = 5.6 Hz, 1H), 4.07 (t, *J* = 6.7 Hz, 2H), 3.07 (d, *J* = 5.7 Hz, 2H), 2.54 (s, 3H), 1.56 – 1.44 (m, 2H), 1.24 (dq, *J* = 14.8, 7.4 Hz, 2H), 0.86 (t, *J* = 7.4 Hz, 3H). ^{13}C NMR (100 MHz, $CDCl_3$) δ 169.3, 166.9, 138.3, 135.0, 135.0, 134.4, 132.3, 132.3, 131.8, 129.2, 122.1, 118.0, 116.1, 65.3, 55.0, 39.8, 30.5, 19.1, 16.9, 13.7. mp: 73−75 °C. HRMS (ESI): m/z ($M+H^+$) calcd for $C_{22}H_{23}O_5N_2S$, 427.1322, found: 427.1329.

Butyl 2-(7-methyl-1,1-dioxido-2-(3-(trifluoromethyl)benzoyl)-2,3-dihydrobenzo[d]isothiazol-3-yl)acetate (**14k**). (43.1 mg, 92% yield). ^{1}H NMR (400 MHz, $CDCl_3$) δ 8.17 – 8.07 (m, 2H), 7.86 (d, *J* = 7.8 Hz, 1H), 7.65 (t, *J* = 7.7 Hz, 1H), 7.59 (t, *J* = 7.6 Hz, 1H), 7.40 (d, *J* = 7.7 Hz, 1H), 7.33 (d, *J* = 7.5 Hz, 1H), 6.12 (t, *J* = 5.6 Hz, 1H), 4.09 (t, *J* =

6.7 Hz, 2H), 3.08 (d, *J* = 5.7 Hz, 2H), 2.55 (s, 3H), 1.57 – 1.47 (m, 2H), 1.26 (dq, *J* = 14.9, 7.3 Hz, 2H), 0.87 (t, *J* = 7.3 Hz, 3H). ^{13}C NMR (100 MHz, $CDCl_3$) δ 169.5, 167.3, 135.3, 135.2, 135.0, 134.3, 132.5, 131.9, 131.7, 131.2 (q, *J* = 33.0 Hz), 129.3 (dd, *J* = 7.2, 3.5 Hz), 129.1, 125.9 (q, *J* = 3.8 Hz), 123.7 (d, *J* = 272.6 Hz), 122.1, 65.4, 55.0, 40.0, 30.5, 19.1, 16.9, 13.7. HRMS (ESI): m/z ($M+H^+$) calcd for $C_{22}H_{23}O_5NF_3S$, 470.1244, found: 470.1245.

Butyl 2-(7-methyl-1,1-dioxido-2-(2-(trifluoromethyl)benzoyl)-2,3-dihydrobenzo[d]isothiazol -3-yl)acetate (**14l**). (42.2 mg, 90% yield). ^{1}H NMR (400 MHz, $CDCl_3$) δ 7.82 – 7.73 (m, 2H), 7.72 – 7.64 (m, 2H), 7.58 (t, *J* = 7.7 Hz, 1H), 7.42 (d, *J* = 7.7 Hz, 1H), 7.33 (d, *J* = 7.5 Hz, 1H), 5.99 – 5.90 (m, 1H), 4.11 (t, *J* = 6.7 Hz, 2H), 3.23 (d, *J* = 14.3 Hz, 1H), 3.07 (dd, *J* = 15.0, 6.7 Hz, 1H), 2.53 (s, 3H), 1.59 – 1.50 (m, 2H), 1.27 (dd, *J* = 14.7, 7.2 Hz, 2H), 0.89 (t, *J* = 7.3 Hz, 3H). ^{13}C NMR (100 MHz, $CDCl_3$) δ 169.6, 165.3, 135.04 (d, *J* = 5.3 Hz), 134.3, 132.5, 132.0, 131.7, 131.4, 131.3, 129.2, 127.0 (q, *J* = 3.9 Hz), 122.3, 122.2 (d, *J* = 9.3 Hz), 65.3, 55.2, 39.4, 30.6, 19.1, 17.0, 13.8. mp: 84−85 °C. HRMS (ESI): m/z ($M+H^+$) calcd for $C_{22}H_{23}O_5NF_3S$, 470.1244, found: 470.1239.

General synthetic procedure of compound **14m-14u**. Et_3N (3.0 equivalent, 41 mg) and 4-(Trifluoromethylbenzoylchloride (1.5 equivalent) was added to a solution of compound **11** (0.1 mmol) in 1 mL of DCM, and the reaction mixture was stirred at room temperature and monitored by LCMS until all of the starting material was consumed completely. Solvent was removed *in vacuo*, and the residue was diluted

with 10 mL of ethyl acetate, washed with 10 mL water, and extracted with ethyl acetate two times. Then the organic phase was combined, washed with brine, and dried over anhydrous Na_2SO_4. The organic layer was concentrated and purified with column chromatography on silica gel to afford compounds **14m-14u**.

Butyl 2-(5,7-dimethyl-1,1-dioxido-2-(4-(trifluoromethyl)benzoyl)-2,3-dihydrobenzo[d]isothiazol-3-yl)acetate (**14m**). (41.5 mg, 86% yield). ^{1}H NMR (400 MHz, $CDCl_3$) δ 7.99 (d, *J* = 8.1 Hz, 2H), 7.76 (d, *J* = 8.0 Hz, 2H), 7.18 (s, 1H), 7.14 (s, 1H), 6.06 (t, *J* = 5.6 Hz, 1H), 4.16 – 4.03 (m, 2H), 3.06 (d, *J* = 5.7 Hz, 2H), 2.50 (s, 3H), 2.44 (s, 3H), 1.59 – 1.46 (m, 2H), 1.31 – 1.22 (m, 2H), 0.87 (t, *J* = 7.4 Hz, 3H). ^{13}C NMR (100 MHz, $CDCl_3$) δ 169.5, 167.4, 145.6, 137.8, 135.4, 134.6, 134.1 (q, *J* = 32.8 Hz), 132.7, 129.8, 129.1, 125.5 (q, *J* = 3.7 Hz), 125.1, 122.4, 65.3, 54.9, 40.0, 30.6, 21.9, 19.1, 16.9, 13.8. mp: 91−92 °C. HRMS (ESI): m/z ($M+H^+$) calcd for $C_{23}H_{25}O_5NF_3S$, 484.1400, found: 484.1406.

Butyl 2-(6,7-dimethyl-1,1-dioxido-2-(4-(trifluoromethyl)benzoyl)-2,3-dihydrobenzo[d]isothiazol-3-yl)acetate (**14n**). (45.3 mg, 90% yield). ^{1}H NMR (400 MHz, $CDCl_3$) δ 7.98 (d, *J* = 8.2 Hz, 2H), 7.78 (d, *J* = 8.1 Hz, 2H), 7.67 (d, *J* = 8.3 Hz, 1H), 7.39 (d, *J* = 8.2 Hz, 1H), 6.08 (t, *J* = 5.7 Hz, 1H), 4.09 (t, *J* = 6.9 Hz, 2H), 3.07 (d, *J* = 5.3 Hz, 2H), 2.56 (s, 3H), 1.58 – 1.49 (m, 2H), 1.30 – 1.22 (m, 2H), 0.88 (t, *J* = 7.4 Hz, 3H). ^{13}C NMR (100 MHz, $CDCl_3$) δ 169.3, 167.2, 137.5, 136.8, 135.0, 134.5, 134.3, 134.2, 133.7, 133.0, 129.1, 125.6 (q, *J* = 3.6 Hz), 123.7 (d, *J* = 271 Hz), 123.3, 65.5, 54.3, 39.7, 30.6, 19.1,

14.7, 13.8. mp: 98−99 °C.

Butyl 2-(5-fluoro-7-methyl-1,1-dioxido-2-(4-(trifluoromethyl)benzoyl)-2,3-dihydrobenzo[d]isothiazol-3-yl)acetate (**14o**). (42.4 mg, 87% yield). ^{1}H NMR (400 MHz, $CDCl_3$) δ 7.98 (d, *J* = 7.7 Hz, 2H), 7.77 (d, *J* = 7.7 Hz, 2H), 7.13 (d, *J* = 7.9 Hz, 1H), 7.06 (d, *J* = 8.9 Hz, 1H), 6.09 (s, 1H), 4.11 (t, *J* = 6.6 Hz, 2H), 3.14 – 3.01 (m, 2H), 2.55 (s, 3H), 1.55 – 1.50 (m, 2H), 1.32 – 1.24 (m, 2H), 0.89 (t, *J* = 7.1 Hz, 3H). ^{13}C NMR (100 MHz, $CDCl_3$) δ 169.3, 167.2, 138.3, 137.5, 129.1, 128.6, 125.7, 125.6, 119.6, 119.4, 109.8, 109.5, 100.1, 65.5, 54.7, 39.7, 30.6, 19.2, 17.1, 13.8. mp: 65−67 °C. HRMS (ESI): m/z ($M+H^+$) calcd for $C_{22}H_{22}O_5NF_4S$, 488.1149, found: 488.1137.

Butyl 2-(4-fluoro-7-methyl-1,1-dioxido-2-(4-(trifluoromethyl)benzoyl)-2,3-dihydrobenzo[d]isothiazol-3-yl)acetate (**14p**). (41.9 mg, 86% yield). ^{1}H NMR (400 MHz, $CDCl_3$) δ 8.00 (d, *J* = 8.1 Hz, 2H), 7.78 (d, *J* = 8.2 Hz, 2H), 7.37 – 7.24 (m, 2H), 6.18 (t, *J* = 4.9 Hz, 1H), 4.04 (t, *J* = 6.7 Hz, 2H), 3.22 (dd, *J* = 14.9, 4.4 Hz, 1H), 3.10 (dd, *J* = 14.9, 5.5 Hz, 1H), 2.51 (s, 3H), 1.53 – 1.40 (m, 2H), 1.26 – 1.16 (m, 2H), 0.85 (t, *J* = 7.4 Hz, 3H). ^{13}C NMR (100 MHz, $CDCl_3$) δ 168.8, 167.3, 157.2, 154.7, 137.5, 134.4 (d, *J* = 32.6 Hz), 134.3 (d, *J* = 3.8 Hz), 133.8 (d, *J* = 6.6 Hz), 130.7 (d, *J* = 4.4 Hz), 129.2, 125.6 (q, *J* = 3.7 Hz), 123.7 (d, *J* = 272.8 Hz), 122.1 (d, *J* = 19.6 Hz), 120.7 (d, *J* = 19.7 Hz), 65.3, 52.5 (d, *J* = 1.8 Hz), 37.9 (d, *J* = 1.7 Hz), 30.4, 19.0, 16.2, 13.7. mp: 101−102 °C. HRMS (ESI): m/z ($M+H^+$) calcd for $C_{22}H_{22}O_5NF_4S$, 488.1149, found: 488.1151.

Butyl 2-(7-chloro-1,1-dioxido-2-(4-(trifluoromethyl)benzoyl)-2,3-dihydrobenzo[d]isothiazol-3-yl)acetate (**14q**). (41.6 mg, 85% yield). ^{1}H NMR (400 MHz, $CDCl_3$) δ 7.98 (d, *J* = 8.1 Hz, 2H), 7.77 (d, *J* = 8.2 Hz, 2H), 7.64 (t, *J* = 7.8 Hz, 1H), 7.52 (d, *J* = 7.9 Hz, 2H), 6.12 (t, *J* = 5.7 Hz, 1H), 4.16 – 4.03 (m, 2H), 3.09 (d, *J* = 5.8 Hz, 2H), 1.51 (dp, *J* = 13.5, 6.8 Hz, 2H), 1.30 – 1.20 (m, 2H), 0.87 (t, *J* = 7.4 Hz, 3H). ^{13}C NMR (101 MHz, $CDCl_3$) δ 169.1, 167.1, 137.7, 137.5, 135.4, 134.2 (q, *J* = 32.8 Hz), 131.9, 131.0, 129.3, 129.0, 125.6, 125.6, 125.5, 125.5, 123.6 (d, *J* = 271.2 Hz), 123.2, 65.4, 54.5, 39.5, 30.4, 19.0, 13.6. mp: 70−72 °C.

Butyl 2-(4,7-dimethoxy-1,1-dioxido-2-(4-(trifluoromethyl)benzoyl)-2,3-dihydrobenzo[d]isothiazol-3-yl)acetate (**14r**). (47.9 mg, 93% yield). ^{1}H NMR (400 MHz, $CDCl_3$) δ 7.98 (d, *J* = 8.1 Hz, 2H), 7.74 (d, *J* = 8.2 Hz, 2H), 7.08 (d, *J* = 8.9 Hz, 1H), 6.93 (d, *J* = 8.9 Hz, 1H), 6.11 – 6.02 (m, 1H), 4.02 (t, *J* = 6.6 Hz, 2H), 3.91 (s, 3H), 3.87 (s, 3H), 3.19 (dd, *J* = 14.6, 4.2 Hz, 1H), 3.11 (dd, *J* = 14.6, 5.8 Hz, 1H), 1.52 – 1.43 (m, 2H), 1.23 (dd, *J* = 14.5, 7.2 Hz, 2H), 0.85 (t, *J* = 7.4 Hz, 3H). ^{13}C NMR (100 MHz, $CDCl_3$) δ 169.5, 167.5, 148.8, 148.5, 138.0, 134.0 (q, *J* = 32.5 Hz), 129.2, 125.5 (q, *J* = 3.6 Hz), 124.7, 123.8 (d, *J* = 271.0 Hz), 122.4, 116.7, 112.7, 65.1, 56.6, 56.4, 53.6, 37.4, 30.5, 19.1, 13.8. mp: 85−87 °C. HRMS (ESI): m/z ($M+H^+$) calcd for $C_{23}H_{25}O_7NF_3S$, 516.1298, found: 516.1303.

Butyl 2-(5,7-dimethoxy-1,1-dioxido-2-(4-(trifluoromethyl)benzoyl)-2,3-dihydrobenzo[d]isothiazol

hiazol-3-yl)acetate (**14s**). (46.9 mg, 91% yield). ^{1}H NMR (400 MHz, $CDCl_3$) δ 7.96 (d, *J* = 8.1 Hz, 2H), 7.74 (d, *J* = 8.2 Hz, 2H), 6.57 (s, 1H), 6.46 (s, 1H), 6.03 (t, *J* = 5.8 Hz, 1H), 4.11 (t, *J* = 6.7 Hz, 2H), 3.89 (s, 3H), 3.87 (s, 3H), 3.10 – 2.99 (m, 2H), 1.59 – 1.52 (m, 2H), 1.34 – 1.25 (m, 2H), 0.88 (t, *J* = 7.4 Hz, 3H). ^{13}C NMR (100 MHz, $CDCl_3$) δ 169.6, 167.4, 166.7, 156.8, 139.1, 137.9, 133.9 (d, *J* = 32.8 Hz), 129.02, 125.4 (q, *J* = 3.6 Hz), 123.8 (d, *J* = 272.7 Hz), 114.5, 100.0, 99.7, 65.4, 56.4, 56.2, 55.0, 40.1, 30.6, 19.2, 13.8. mp: 116−117 °C. HRMS (ESI): m/z ($M+H^+$) calcd for $C_{23}H_{25}O_7NF_3S$, 516.1298, found: 516.1304.

Butyl 3-(2-butoxy-2-oxoethyl)-2-(4-(trifluoromethyl)benzoyl)-2,3-dihydrobenzo[d]isothiazol e-7-carboxylate 1,1-dioxide (**14t**). (49.9 mg, 90% yield). ^{1}H NMR (400 MHz, $CDCl_3$) δ 8.20 (d, *J* = 6.5 Hz, 1H), 7.98 (d, *J* = 8.1 Hz, 2H), 7.83 (dd, *J* = 13.7, 7.3 Hz, 2H), 7.75 (d, *J* = 8.2 Hz, 2H), 6.17 (t, *J* = 5.8 Hz, 1H), 4.41 – 4.31 (m, 2H), 4.10 (t, *J* = 6.7 Hz, 2H), 3.16 – 3.04 (m, 2H), 1.76 – 1.67 (m, 2H), 1.57 – 1.49 (m, 2H), 1.40 (dt, *J* = 13.8, 6.9 Hz, 2H), 1.31 – 1.21 (m, 2H), 0.94 – 0.85 (m, 6H). ^{13}C NMR (100 MHz, $CDCl_3$) δ 169.5, 167.6, 162.6, 137.9, 137.3, 134.4, 134.2, 134.0 (d, *J* = 32.8 Hz), 132.1, 129.5, 129.0, 127.4, 126.8, 125.5 (q, *J* = 3.7 Hz), 66.8, 65.5, 54.0, 40.0, 30.6, 30.5, 19.2, 19.1, 13.8, 13.7. mp: 91−92 °C. HRMS (ESI): m/z ($M+H^+$) calcd for $C_{26}H_{29}O_7NF_3S$, 556.1611, found: 556.1609.

Butyl (E)-3-(3-(2-butoxy-2-oxoethyl)-5-methyl-1,1-dioxido-2-(4-(trifluoromethyl)benzoyl)-2, 3-dihydrobenzo[d]isothiazol-7-yl)acrylate (**14u**). (52.9 mg, 89% yield). ^{1}H NMR (400

MHz, $CDCl_3$) δ 7.98 (d, *J* = 8.1 Hz, 2H), 7.89 (d, *J* = 15.9 Hz, 1H), 7.77 (d, *J* = 8.2 Hz, 2H), 7.54 (s, 1H), 7.38 (s, 1H), 6.56 (d, *J* = 15.9 Hz, 1H), 6.11 (t, *J* = 5.7 Hz, 1H), 4.17 (t, *J* = 6.7 Hz, 2H), 4.10 (t, *J* = 6.7 Hz, 2H), 3.08 (d, *J* = 5.7 Hz, 2H), 2.50 (s, 3H), 1.69 – 1.59 (m, 2H), 1.57 – 1.49 (m, 2H), 1.37 (dq, *J* = 14.7, 7.4 Hz, 2H), 1.27 (dq, *J* = 14.9, 7.5 Hz, 2H), 0.94 – 0.84 (m, 6H). ^{13}C NMR (100 MHz, $CDCl_3$) δ 169.4, 167.2, 165.5, 145.8, 137.6, 136.2, 135.6, 134.29 (d, *J* = 32.9 Hz), 131.2, 130.0, 129.1, 129.0, 126.1, 125.61 (q, *J* = 3.6 Hz), 124.9, 123.7 (d, *J* = 271.1 Hz) 65.4, 65.1, 54.8, 39.9, 30.7, 30.6, 22.0, 19.2, 19.1, 13.8, 13.7. HRMS (ESI): m/z ($M+H^+$) calcd for $C_{29}H_{33}O_7NF_3S$, 596.1924, found: 596.1933.

Methyl 2-(7-methyl-1,1-dioxido-2-(4-(trifluoromethyl)benzoyl)-2,3-dihydrobenzo[d]isothiazol -3-yl)acetate (**14v**). (35.0 mg, 82% yield). ^{1}H NMR (400 MHz, $CDCl_3$) δ 7.99 (d, *J* = 8.1 Hz, 2H), 7.78 (d, *J* = 8.2 Hz, 2H), 7.59 (t, *J* = 7.7 Hz, 1H), 7.39 (d, *J* = 7.6 Hz, 1H), 7.34 (d, *J* = 7.5 Hz, 1H), 6.12 (t, *J* = 5.8 Hz, 1H), 3.69 (s, 3H), 3.08 (d, *J* = 5.9 Hz, 2H), 2.56 (s, 3H). ^{13}C NMR (100 MHz, $CDCl_3$) δ 169.8, 167.4, 137.7, 135.1, 135.0, 134.4, 134.2 (q, *J* = 32.8 Hz), 132.4, 131.9, 129.0, 125.6 (q, *J* = 3.7 Hz), 123.7 (d, *J* = 272.9 Hz), 122.1, 54.9, 52.4, 39.8, 17.0. mp: 138−140 °C.

Tert-butyl 2-(7-methyl-1,1-dioxido-2-(4-(trifluoromethyl)benzoyl)-2,3-dihydrobenzo[d]isothiazol -3-yl)acetate (**14w**). (46.7 mg, 91% yield). ^{1}H NMR (400 MHz, $CDCl_3$) δ 8.00 (d, *J* = 8.1 Hz, 2H), 7.77 (d, *J* = 8.0 Hz, 2H), 7.58 (t, *J* = 7.7 Hz, 1H), 7.42 (d, *J* = 7.8 Hz, 1H), 7.33 (d, *J* = 7.5 Hz, 1H), 6.10 (t, *J* = 5.8 Hz, 1H), 3.04 (dd, *J* = 15.4, 5.0 Hz, 1H),

2.96 (dd, *J* = 15.5, 6.6 Hz, 1H), 2.55 (s, 3H), 1.39 (s, 9H). ^{13}C NMR (100 MHz, $CDCl_3$) δ 168.6, 167.4, 137.9, 135.5, 134.9, 134.2, 134.3 (q, *J* = 32.6 Hz) 132.4, 131.6, 129.1, 125.6 (q, *J* = 3.7 Hz), 123.7 (d, *J* = 272.8 Hz), 122.3, 82.2, 55.1, 41.2, 28.0, 16.9. mp: 120−122 °C. HRMS (ESI): m/z ($M+H^+$) calcd for $C_{22}H_{23}O_5NF_3S$, 470.1244, found: 470.1249.

synthesis of 2-(7-methyl-1,1-dioxido-2-(4-(trifluoromethyl)benzoyl)-2,3-dihydrobenzo[d]isothiazol -3-yl)acetic acid (**15a**). Compound **14w** was added to a solution of DCM /TFA (v/v = 10/1), and the reaction mixture was stirred for 1h at room temperature. then evaporated under reduced pressure to give product **15a** without further purified.

General synthetic procedure of compound **16a-16d**. Oxalyl chloride (4.0 equivalent, 33.8 μL) and DMF (cat.) was added to a solution of compound **15** (0.1 mmol) in 10 mL of DCM, and the reaction mixture was stirred at room temperature and monitored by LCMS until all of the starting material was consumed completely. Solvent was removed *in vacuo*, and the residue was diluted with 2 mL of DCM, and then was added to a solution of corresponding amine (3.0 equivalent) and Et_3N (3.0 equivalent), the reaction mixture was stirred at room temperature and monitored by LCMS until all of the starting material was consumed completely. Solvent was removed *in vacuo*, and washed with 10 mL water, and extracted with ethyl acetate two times. Then the organic phase was combined, washed with brine, and dried over anhydrous Na_2SO_4. The organic layer was concentrated and purified with column chromatography on silica gel to afford compound **16a-16d**.

2-(7-methyl-1,1-dioxido-2-(4-(trifluoromethyl)benzoyl)-2,3-dihydrobenzo[d]isothiazol-3-yl)acetamide (**16a**). (33.7 mg, 82% yield). ^{1}H NMR (400 MHz, CD_3OD) δ 8.03 (d, *J* = 8.1 Hz, 2H), 7.83 (d, *J* = 8.2 Hz, 2H), 7.66 (t, *J* = 7.7 Hz, 1H), 7.52 (d, *J* = 7.8 Hz, 1H), 7.43 (d, *J* = 7.5 Hz, 1H), 6.17 (t, *J* = 6.3 Hz, 1H), 2.99 (dd, *J* = 14.6, 5.5 Hz, 1H), 2.88 (dd, *J* = 14.6, 7.1 Hz, 1H), 2.51 (s, 3H). ^{13}C NMR (101 MHz, CD_3OD) δ 173.7, 168.5, 139.7, 137.0, 135.6, 135.5, 134.7 (d, *J* = 32.5 Hz), 133.5, 132.7, 130.4, 126.3 (d, *J* = 3.8 Hz), 125.2 (d, *J* = 270.2 Hz), 123.7, 56.6, 41.8, 16.7. mp: 177−178 °C. HRMS (ESI): m/z ($M+H^+$) calcd for $C_{18}H_{16}O_4N_2F_3S$, 413.0777, found: 413.0775.

N-butyl-2-(7-methyl-1,1-dioxido-2-(4-(trifluoromethyl)benzoyl)-2,3-dihydrobenzo[d]isothiazol-3-yl)acetamide (**16b**). (40.2 mg, 86% yield). ^{1}H NMR (400 MHz, $CDCl_3$) δ 7.98 (d, *J* = 8.0 Hz, 2H), 7.77 (d, *J* = 8.0 Hz, 2H), 7.57 (t, *J* = 7.7 Hz, 1H), 7.48 (d, *J* = 7.7 Hz, 1H), 7.32 (d, *J* = 7.4 Hz, 1H), 6.17 (dd, *J* = 7.6, 4.6 Hz, 1H), 5.61 (s, 1H), 3.26 (dd, *J* = 13.2, 6.6 Hz, 2H), 3.05 (dd, *J* = 14.5, 4.4 Hz, 1H), 2.76 (dd, *J* = 14.5, 8.0 Hz, 1H), 2.55 (s, 3H), 1.49 – 1.39 (m, 2H), 1.33 – 1.23 (m, 2H), 0.89 (t, *J* = 7.3 Hz, 3H). ^{13}C NMR (100 MHz, $CDCl_3$) δ 168.1, 167.1, 137.8, 135.7, 134.8, 134.4, 134.0, 132.3, 131.7, 129.0, 125.6 (q, *J* = 3.7 Hz), 123.7 (d, *J* = 271 Hz), 122.7, 55.6, 42.3, 39.6, 31.7, 20.1, 17.0, 13.8. mp: 188−189 °C. HRMS (ESI): m/z ($M+H^+$) calcd for $C_{22}H_{24}O_4N_2F_3S$, 469.1403, found: 469.1403.

N,N-dibutyl-2-(7-methyl-1,1-dioxido-2-(4-(trifluoromethyl)benzoyl)-2,3-dihydrobenzo[d]isothiazol-3-yl)acetamide (**16c**). (46.1 mg, 88% yield). ^{1}H NMR (400 MHz, $CDCl_3$) δ 7.99 (d, *J* = 8.1 Hz, 2H), 7.77 (d, *J* = 8.2 Hz, 2H), 7.56 (dt, *J* = 15.2, 7.8 Hz,

2H), 7.31 (d, *J* = 7.3 Hz, 1H), 6.35 (dd, *J* = 8.6, 4.1 Hz, 1H), 3.43 – 3.28 (m, 2H), 3.27 – 3.07 (m, 3H), 2.94 (dd, *J* = 15.4, 8.7 Hz, 1H), 2.55 (s, 3H), 1.57 – 1.35 (m, 4H), 1.34 – 1.21 (m, 4H), 0.94 – 0.86 (m, 6H).^{13}C NMR (101 MHz, $CDCl_3$) δ 168.1, 166.8, 138.0, 136.4, 134.5, 134.2, 133.9 (q, *J* = 32.6 Hz), 132.2, 131.5, 128.8, 125.5 (q, *J* = 3.6 Hz), 123.7 (q, *J* = 271.1 Hz), 123.3, 55.8, 47.9, 46.1, 39.2, 31.2, 29.9, 20.3, 20.1, 16.9, 14.0, 13.8.

2-(7-methyl-1,1-dioxido-2-(4-(trifluoromethyl)benzoyl)-2,3-dihydrobenzo[d]isothiazol-3-yl)-N-phenylacetamide (**16d**). (41.0 mg, 84% yield). ^{1}H NMR (400 MHz, DMSO) δ 10.12 (s, 1H), 7.96 (q, *J* = 8.4 Hz, 4H), 7.73 (t, *J* = 7.7 Hz, 1H), 7.52 (dt, *J* = 12.4, 6.4 Hz, 4H), 7.28 (t, *J* = 7.9 Hz, 2H), 7.04 (t, *J* = 7.4 Hz, 1H), 6.18 (t, *J* = 6.0 Hz, 1H), 3.13 – 3.02 (m, 2H), 2.46 (s, 3H). ^{13}C NMR (101 MHz, DMSO) δ 166.82, 166.46, 138.68, 138.20, 135.70, 134.54, 133.51, 132.05 (d, *J* = 32.1 Hz), 131.47, 131.39, 129.09, 128.72, 125.46 (q, *J* = 3.6 Hz), 123.7 (q, *J* = 271.1 Hz), 123.51, 122.68, 119.41, 55.46, 41.77, 16.10.

Syntheis of butyl (E)-2-(7-methyl-1,1-dioxido-2-(4-(trifluoromethyl)benzoyl)benzo[d]isothiazol-3(2H)-ylidene)acetate (**18**). To a solution of compound **10a** (0.5 mmol, 30mg) in 1 mL DMF was added Cs_2CO_3 (2.0 equivalent, 65.4 mg), the reaction mixture was heated to 120□ and monitored by LCMS until all of the starting material was consumed completely. Solvent was removed *in vacuo*, and the residue was diluted with 10 ml ethyl acetate, washed with 10 ml water, and extracted with ethyl acetate for two times. Then the organic phase was combined, washed with brine and dried with anhydrous Na_2SO_4.

The organic layer was concentrated, and purified with column chromatography on silica gel to afford intermediate **17** (75% yield). *Butyl (E)-2-(7-methyl-1,1-dioxidobenzo[d]isothiazol-3(2H)-ylidene)acetate* (**17**) ^{1}H NMR (400 MHz, $CDCl_3$) δ 10.13 (s, 1H), 7.59 – 7.55 (m, 2H), 7.45 (d, *J* = 6.7 Hz, 1H), 5.67 (s, 1H), 4.21 (t, *J* = 6.7 Hz, 2H), 2.68 (s, 3H), 1.71 – 1.64 (m, 3H), 1.43 (dq, *J* = 14.7 Hz, 7.4 Hz, 3H), 0.96 (t, *J* = 7.4 Hz, 3H). ^{13}C NMR (100 MHz, $CDCl_3$) δ 168.8, 143.7, 135.0, 134.4, 133.6, 132.7, 129.1, 119.8, 88.4, 64.8, 30.9, 19.3, 17.2, 13.9. HRMS (ESI): *m/z* ($M + Na^+$) calcd for $C_{14}H_{17}NNaO_4S$, 318.0770, found:318.0776.

Et_3N (3.0 equivalent, 41 mg) and 4-(Trifluoromethylbenzoylchloride (1.5 equivalent) was added to a solution of intermediate **17** (0.1 mmol) in 1 mL of DCM, and the reaction mixture was stirred at room temperature and monitored by LCMS until all of the starting material was consumed completely. Solvent was removed *in vacuo*, and the residue was diluted with 10 mL of ethyl acetate, washed with 10 mL water, and extracted with ethyl acetate two times. Then the organic phase was combined, washed with brine, and dried over anhydrous Na_2SO_4. The organic layer was concentrated and purified with column chromatography on silica gel to afford compound **18**. (43.4 mg, 93% yield) ^{1}H NMR (400 MHz, $CDCl_3$) δ 8.22 (d, *J* = 7.1 Hz, 1H), 8.11 (d, *J* = 7.7 Hz, 1H), 7.82 – 7.68 (m, 2H), 7.43 (d, *J* = 7.4 Hz, 1H), 7.37 (t, *J* = 7.7 Hz, 1H), 7.23 (d, *J* = 7.7 Hz, 1H), 4.10 (t, *J* = 6.1 Hz, 2H), 2.69 (s, 3H), 1.40 – 1.30 (m, 2H), 0.95 (dt, *J* = 14.5, 7.3 Hz, 2H), 0.70 (t, *J* = 7.3 Hz, 3H). ^{13}C NMR (100 MHz, $CDCl_3$) δ 166.8, 165.5, 143.6, 135.4, 134.9, 134.9, 133.6, 133.1, 130.6, 130.6, 129.5, 126.1 (q, *J* = 2.9 Hz), 125.5, 125.5, 123.4, 65.6, 30.2, 18.7, 17.1, 13.3.

Synthesis of (3-(2-butoxyethyl)-7-methyl-1,1-dioxidobenzo[d]isothiazol-2(3H)-yl)(4-(trifluoromethyl)phenyl)methanone(**21**). Compound **10a** (1 mmol, 297 mg) was dissolved in THF (1 mL) and then added dropwise to an ice bath cooled solution of THF (1 mL) which contained lithium aluminum hydride (76 mg, 2.0 equivalent), then the reaction mixture was stirred for 16 hours at room temperature, when the starting material was consumed completely, cooled to 0 °C and 10% H_2SO_4 aqueous solution was added until no bubbles were generated. The mixture was filtered through a pad, THF was removed by evaporation and the resulting oil was redissolved in ethyl acetate (30 mL), washed with $NaHCO_3$ solution (20 mL) and brine (20 mL), and dried over anhydrous Na_2SO_4. The organic layer was concentrated and purified with column chromatography on silica gel to afford 3-(2-hydroxyethyl)-7-methyl-2,3-dihydrobenzo[d]isothiazole 1,1-dioxide (**19**). 4-(Trifluoromethyl) benzoic acid (1.1 equivalent, 104.5 mg), EDCI (1.1 equivalent, 105.5 mg), HOBt (1.1 equivalent, 74.5 mg) and DIPEA (1.1 equivalent, 70.9 mg) were added to a solution of intermediate **19** (0.5 mmol, 113.5 mg) in 10 mL of DCM, the reaction mixture was stirred at room temperature and monitored by LCMS until all of the starting material was consumed completely. Solvent was removed *in vacuo*, extracted with ethyl acetate two times, washed with 10 mL water. Then the organic phase was combined, washed with brine, and dried over anhydrous Na_2SO_4. The organic layer was concentrated and purified with column chromatography on silica gel to afford

(3-(2-hydroxyethyl)-7-methyl-1,1-dioxidobenzo[d]isothiazol-2(3H)-yl)(4-(trifluorome thyl)phenyl)methanone (**20**). K_2CO_3 (3.0 equivalent, 41.4 mg) and 1-iodobutane (1.5 equivalent, 27.6 mg) were added to a solution of intermediate **20** (0.1 mmol, 39.9 mg) in 1 mL of acetone, the reaction mixture was stirred at room temperature and monitored by LCMS until all of the starting material was consumed completely. Solvent was removed *in vacuo*, extracted with ethyl acetate, washed with 10 mL water. Then the organic phase was combined, washed with brine, and dried over anhydrous Na_2SO_4. The organic layer was concentrated and purified with column chromatography on silica gel to afford compound **21**. (34.1 mg, 75% yield) ^{1}H NMR (400 MHz, $CDCl_3$) δ 7.87 (d, *J* = 8.1 Hz, 2H), 7.62 (d, *J* = 8.1 Hz, 2H), 7.41 (t, *J* = 7.6 Hz, 1H), 7.19 (dd, *J* = 11.5, 7.8 Hz, 2H), 4.63 (s, 1H), 4.47 (dt, *J* = 11.6, 5.9 Hz, 1H), 4.34 – 4.26 (m, 1H), 3.42 (dt, *J* = 14.3, 7.5 Hz, 1H), 3.35 – 3.26 (m, 1H), 2.61 (s, 3H), 2.54 – 2.47 (m, 1H), 2.45 – 2.36 (m, 1H), 1.82 – 1.72 (m, 2H), 1.50 – 1.38 (m, 2H), 0.96 (t, *J* = 7.4 Hz, 3H). ^{13}C NMR (100 MHz, $CDCl_3$) δ 165.1, 137.4, 134.6 (d, *J* = 32.4 Hz), 134.6, 133.6, 133.1, 132.8, 130.8, 130.0, 125.30 (q, *J* = 3.7 Hz), 123.7 (d, *J* = 272.7 Hz), 121.1, 60.9, 58.4, 43.7, 31.3, 30.5, 20.4, 16.9, 13.8. HRMS (ESI): m/z ($M+H^+$) calcd for $C_{22}H_{25}O_4NF_3S$, 456.1451, found: 456.1443.

Synthesis of (3-((3-butyl-1,2,4-oxadiazol-5-yl)methyl)-7-methyl-1,1-dioxidobenzo[d]isothiazol-2(3 H)-yl)(3-(trifluoromethyl)phenyl)methanone (**23**). Oxalyl chloride (4.0 equivalent, 338 μL) and DMF (cat.) was added to a solution of compound **15** (1.0 mmol) in 10 mL of DCM, and the reaction mixture was stirred at room temperature and monitored

by LCMS until all of the starting material was consumed completely. Solvent was removed *in vacuo,* and the residue was diluted with 2 mL of DCM, and then was added to a solution of corresponding amine (3.0 equivalent) and Et_3N (3.0 equivalent), the reaction mixture was stirred at room temperature and monitored by LCMS until all of the starting material was consumed completely. Solvent was removed *in vacuo*, the residue was dissolved in toluene, and the reaction mixture was stirred at 100 °C and monitored by LCMS until all of the starting material was consumed completely. Solvent was removed *in vacuo,* and the residue was diluted with 10 mL of ethyl acetate, washed with 10 mL water. Then the organic phase was combined, washed with brine, and dried over anhydrous Na_2SO_4. The organic layer was concentrated and purified with column chromatography on silica gel to afford compound **23**. (320.4 mg, 65% yield) ^{1}H NMR (400 MHz, $CDCl_3$) δ 8.00 (d, *J* = 8.1 Hz, 2H), 7.77 (d, *J* = 8.2 Hz, 2H), 7.63 (t, *J* = 7.7 Hz, 1H), 7.36 (dd, *J* = 7.4, 5.0 Hz, 2H), 6.18 (t, *J* = 5.4 Hz, 1H), 3.77 (dd, *J* = 14.8, 5.5 Hz, 1H), 3.53 (dd, *J* = 14.8, 5.5 Hz, 1H), 2.71 – 2.59 (m, 2H), 2.52 (s, 3H), 1.62 – 1.56 (m, 2H), 1.33 – 1.25 (m, 2H), 0.86 (t, *J* = 7.3 Hz, 3H). ^{13}C NMR (100 MHz, $CDCl_3$) δ 174.0, 171.0, 167.4, 137.5, 135.2, 134.5, 134.3 (q, *J* = 32.6 Hz), 133.6, 132.7, 132.2, 129.1, 125.6 (q, *J* = 3.7 Hz), 123.7 (d, *J* = 272.8 Hz) 122.0, 55.7, 32.2, 29.1, 25.6, 22.1, 16.9, 13.8. mp: 88−90 °C.

Synthesis of (3-((5-butyl-1,3,4-oxadiazol-2-yl)methyl)-7-methyl-1,1-dioxidobenzo[d]isothiazol-2(3H)-yl)(3-(trifluoromethyl)phenyl)methanone (**26**). Intermediate **24** was synthesized by the process follow to synthesis of intermediate **22**. Butyric anhydride (2.0 equivalent)

and Et_3N (2.0 equivlent,129.5 μL) was added to a solution of the intermediate (0.5 mmol, 213.5 mg) in 10 mL of THF, and the reaction mixture was stirred at room temperature and monitored by LCMS until all of the starting material was consumed completely. Solvent was removed *in vacuo*, and purified with column chromatography on silica gel to afford 235.1 mg N'-(2-(7-methyl-1,1-dioxido-2-(3-(trifluoromethyl)benzoyl)-2,3-dihydrobenzo[d]isothiazol-3-yl)acetyl)pentanehydrazide (**25**), 92% yield. Then the intermediate was dissolved in DCM, the solution was dropped to a solution of mixture I_2 (2.5 equivalent), PPh_3 (2.5 equivalent), Et_3N (2.5 equivalent), and the reaction mixture was stirred at room temperature and monitored by LCMS until all of the starting material was consumed completely. Solvent was removed *in vacuo*, and purified with column chromatography on silica gel to afford compound **26**. (176.9 mg, 78% yield). ^{1}H NMR (400 MHz, $CDCl_3$) δ 8.13 (s, 1H), 8.10 (d, *J* = 7.9 Hz, 1H), 7.87 (d, *J* = 7.9 Hz, 1H), 7.65 (dd, *J* = 17.1, 7.9 Hz, 2H), 7.40 (d, *J* = 7.8 Hz, 1H), 7.35 (d, *J* = 7.6 Hz, 1H), 6.15 (t, *J* = 4.9 Hz, 1H), 3.77 (dd, *J* = 15.1, 5.0 Hz, 1H), 3.52 (dd, *J* = 15.1, 5.0 Hz, 1H), 2.75 (tq, *J* = 15.4, 7.6 Hz, 2H), 2.50 (s, 3H), 1.66 – 1.57 (m, 2H), 1.35 – 1.28 (m, 2H), 0.87 (t, *J* = 7.3 Hz, 3H). ^{13}C NMR (100 MHz, $CDCl_3$) δ 168.1, 167.3, 161.8, 134.3 (d, *J* = 198.4 Hz), 135.1, 134.5, 132.6, 132.2, 131.9, 131.2 (q, *J* = 33.1 Hz), 129.3 (q, *J* = 3.6 Hz), 129.2, 125.8 (q, *J* = 3.8 Hz), 123.7 (d, *J* = 272.6 Hz), 122.2, 55.9, 30.9, 28.4, 25.1, 22.1, 16.9, 13.6. HRMS (ESI): m/z ($M+H^+$) calcd for $C_{23}H_{23}O_4N_3F_3S$, 494.1356, found: 494.1350.

Synthesis of butyl

2-(7-methyl-1,1-dioxido-2-(4-(trifluoromethyl)benzamido)-2,3-dihydrobenzo[d]isothi azol-3-yl)acetate (**28**). To a solution of compound **11a** (0.5 mmol, 148.5 mg) in 2 mL THF was added NaH (1.2 equivalent, 14.4 mg) at ice bath, then $DppoNH_2$ (1.5 equivalent, 175.5 mg), the reaction mixture was stirred at room temperature and monitored by LCMS until all of the starting material was consumed completely. 10 ml water was added in the mixture, and extracted with ethyl acetate for two times. Then the organic phase was combined, washed with brine and dried with anhydrous Na_2SO_4. The organic layer was concentrated, and purified with column chromatography on silica gel to afford butyl 2-(2-amino-7-methyl-1,1-dioxido-2,3-dihydrobenzo[d]isothiazol-3-yl)acetate (**27)** (29.6 mg, 19% yield). The intermediate **27** was solution in 0.5mL pyridine, then 4-(Trifluoromethyl)benzoylchloride (2.0 equivalent, 39.5 mg) was added. when the starting material was consumed completely, 10 ml 1M HCl aq. was added in the mixture, and extracted with ethyl acetate for two times. Then the organic phase was combined, washed with brine and dried with anhydrous Na_2SO_4. The organic layer was concentrated, and purified with column chromatography on silica gel to afford butyl

2-(7-methyl-1,1-dioxido-2-(4-(trifluoromethyl)benzamido)-2,3-dihydrobenzo[d]isothi azol-3-yl)acetate (**28**). (36.2 mg, 79% yield). ^{1}H NMR (400 MHz, $CDCl_3$) δ 8.51 (s, 1H), 8.00 (d, *J* = 7.9 Hz, 2H), 7.69 (d, *J* = 8.0 Hz, 2H), 7.56 (t, *J* = 7.7 Hz, 1H), 7.35 (d, *J* = 7.6 Hz, 1H), 7.24 (d, *J* = 7.6 Hz, 1H), 5.31 (s, 1H), 4.05 (t, *J* = 6.5 Hz, 2H), 3.09 – 2.93 (m, 2H), 2.68 (s, 3H), 1.57 – 1.47 (m, 2H), 1.27 (dq, *J* = 14.6, 7.3 Hz, 2H),

0.87 (t, *J* = 7.3 Hz, 3H). ^{13}C NMR (100 MHz, $CDCl_3$) δ 170.8, 165.9, 136.0, 135.2, 135.2, 135.1, 133.9, 131.4, 128.3, 126.0, 123.6 (d, *J* = 272.6 Hz), 121.4, 112.4, 65.5, 59.8, 39.5, 30.6, 19.1, 17.4, 13.7. HRMS (ESI): m/z ($M+H^+$) calcd for $C_{22}H_{24}O_5N_2F_3S$, 485.1353, found: 485.1339.

Synthesis of butyl 2-(4-methyl-3-oxo-2-(4-(trifluoromethyl)benzoyl)isoindolin-1-yl)acetate (**31**). A 10 mL sealed tube equipped with a magnetic stir bar was charged with $[RhCp^*Cl_2]_2$ (0.5 mol%, 6 mg), $Cu(OAc)_2$ (2.0 equivalent, 360 mg), $AgSbF_6$ (2 mol%, 7.1 mg), 2-methylbenzamid (135 mg, 1 mmol) and 3.0 mL dioxane. The mixture was stirred, and then butyl acrylate (2.0 equivalent, 218 μL) was added. The reaction tube was capped and stirred at 120 °C. The reaction was monitored by LCMS. When the starting material was consumed completely, solvent was removed under vacuum. The reaction mixture was diluted with ethyl acetate, then washed with 2 N HCl aqueous solution (2 × 20 mL). Subsequently, the mixture was extracted with ethyl acetate (3 × 50 mL). The combined organic layer was washed with brine (20 mL) and then dried over anhydrous sodium sulfate. The organic solvent was removed on a rotary evaporator *in vacuo*. The residue was purified by preparative TLC on silica gel to afford butyl (E)-2-(4-methyl-3-oxoisoindolin-1-ylidene)acetate (**29**). The intermediate **29** was reduced in the presence of Pd/C, H2 then used without further purification. Et_3N (3.0 equivalent, 41 mg) and 4-(Trifluoromethylbenzoylchloride (1.5 equivalent) was added to a solution of intermediate **30** (0.1 mmol) in 1 mL of DCM, and the reaction mixture was stirred at room temperature and monitored by LCMS until all of

the starting material was consumed completely. Solvent was removed *in vacuo*, and the residue was diluted with 10 mL of ethyl acetate, washed with 10 mL water, and extracted with ethyl acetate two times. Then the organic phase was combined, washed with brine, and dried over anhydrous Na_2SO_4. The organic layer was concentrated and purified with column chromatography on silica gel to afford compound **31**. (39.0 mg, 90% yield). ^{1}H NMR (400 MHz, $CDCl_3$) δ 7.80 (d, *J* = 8.0 Hz, 2H), 7.72 (d, *J* = 8.1 Hz, 2H), 7.56 (s, 1H), 7.39 (d, *J* = 7.7 Hz, 1H), 7.28 (s, 1H), 5.70 (t, *J* = 4.6 Hz, 1H), 4.00 (t, *J* = 6.6 Hz, 2H), 3.17 (d, *J* = 4.9 Hz, 2H), 2.62 (s, 3H), 1.49 – 1.34 (m, 2H), 1.21 (dt, *J* = 15.1, 7.5 Hz, 2H), 0.85 (t, *J* = 7.4 Hz, 3H). ^{13}C NMR (100 MHz, $CDCl_3$) δ 169.6, 169.2, 167.3, 145.2, 140.2, 138.5, 134.1, 133.3, 133.0, 131.2, 129.0, 127.1, 124.93 (q, *J* = 7.2, 3.6 Hz), 120.3, 64.7, 55.2, 36.8, 30.47, 19.0, 17.9, 13.6. mp: 69−71 °C. HRMS (ESI): *m/z* (M + H^+) calcd for $C_{23}H_{23}O_4NF_3$, 434.1574, found: 434.1579.

4.2 Biology

4.2.1 Animals.

Male C57BL/6 mice (6−8 weeks old) were purchased from Vital River Experimental Animal Co., Ltd. (Beijing, China). Mice were housed in the specific pathogen-free conditions with a 12h light/dark cycle and free access to food and water in the animal research center laboratory of Tsinghua University. All animal protocols were conducted in compliance with the Institute of Animal Care and Use Committee (IACUC) of Tsinghua University approved by institutional and national guidelines.

4.2.2 Cell culture.

HEK-Blue hNOD1 cells, HEK-Blue hNOD2 cells were purchased from InvivoGen (San Diego, CA) and cultured in Dulbecco's modified Eagle medium (DMEM) (Life Technologies, CA, USA) with 4.5 g/L glucose (Life Technologies), 10% (v/v) fetal bovine serum (FBS) (Gibco, Australia), 1% (v/v) penicillin/streptomycin (Life Technologies), 100 μg/mL Normocin (InvivoGen, San Diego, CA), and additional selective antibiotics according to the manufacturer's protocol. B16F10 cell line was purchased from ATCC (Mannassas, VA, USA) and cultured in DMEM, human monocytic leukemia THP1 cell line was kindly provided by Dr. Wanli Liu (Tsinghua University, Beijing, China) maintained in RPMI-1640 medium (Life Technologies), supplemented with 10% (v/v) FBS, 1% (v/v) penicillin/streptomycin. All the cells were grown at 37 °C in a 5% CO2 humidified incubator and guaranteed to be mycoplasma-free.

4.2.3 Screening assay to identify NOD1/2 dual inhibitors.

HEK-Blue hNOD1 cells were seeded in 96-well plates at 50,000 cells/well, preincubated with compounds (10 μM) for 3 h, and stimulated with 50 ng/mL (~EC_{80}) C12-iE-DAP (InvivoGen, San, Diego, CA) for 20 h. As we previously described [30], HEK-Blue hNOD2 cells were pretreated with different compounds (10 μM) for 3 h and then stimulated with 100 ng/mL (~EC_{80}) MDP (InvivoGen) for an additional 20 h. SEAP was detected using HEK-Blue detection (InvivoGen) and measured by a spectrophotometer at 655 nm according to the manufacturer's instructions. The

inhibition rate (%) was determined using the following formula: inhibition (%) = {[C12-iE-DAP (OD655) or MDP (OD655) – compounds (OD655)] / [C12-iE-DAP (OD655) or MDP (OD655)] × 100. Once the inhibition rate (%) was >50%, compounds were retested, and the SRB assay was conducted to exclude cytotoxicity. The IC50 values were determined using the GraphPad Prism 7 software [30].

4.2.4 Quantitative real-time PCR

The expression of mRNA was determined by quantitative reverse transcriptase-PCR analysis as previously described [30] and normalized to GAPDH. Human IL-6 (Hs00985639_m1) probe and GAPDH (Hs02758991_g1) probe from Applied Biosystems were used for PCR analysis. The data was calculated using the following formula: $2^{-((CT\ sample-CT\ sample\ GAPDH) - (CT\ control-CT\ control\ GAPDH))}$.

4.2.5 Western Blotting.

Cells were lysed in cold whole cell lysis buffer and the protein expression levels were determined as previously described [30]. Antibodies phosphor-p38 (no. 4631), p38 (no. 9212S), phosphor-JNK (no. CST9251S), JNK (no. 9252S), phosphor-RIP2 (no. 14397S), RIP2 (no. 4142) and IκBα (no. 9242S) were obtained from Cell Signaling Technology (Danvers, USA). Phosphor-ERK1/2 (sc-7383) and ERK1/2 (sc-94) antibodies were purchased from Santa Cruz Biotechnology (Santa Cruz, CA). Anti-beta Actin antibody (HRP) (ab49900), goat polyclonal secondary antibody to rabbit IgG-H&L-HRP (ab6721) and rabbit polyclonal secondary antibody to mouse IgG-H&L-HRP (ab6728) were from Abcam (Cambrige, UK). The protein bands were

developed by chemiluminescence (Thermo Scientific, Rockford, USA) with ChemiDoc XRS+ (Bio-Rad).

4.2.6 MDP-Induced Mice Challenge Model.

Male C57BL/6 mice (n =10/treatment group) were *iv.* injected with vehicle or **14k** (50mg/kg) 2 min prior to MDP challenge (4mg/kg, *ip.*). At 2 h post MDP challenge, mice were sacrificed and terminal serum was prepared from blood. Serum KC level was quantified by ELISA (RD, MKC00B).

4.2.7 Statistical Analysis.

Statistical analyses were performed by two tailed Student's *t*-test, *P* values are indicated in the figure with statistically significant ($P < 0.05$). All results were confirmed in at least three independent experiments. All quantitative data were statistical analyzed with GraphPad software7.0.

Declaration of competing interest

The authors declare that they have no known competing financial interests or personal relationships that could have appeared to influence the work reported in this paper.

Acknowledgments

We gratefully acknowledge the funding support of grants from the National Natural Science Foundation of China (Grants 81803358, 81703329, 81273364 and 81773114) and the Non-profit Central Research Institute of Chinese Academy of Medical Sciences (2019-RC-HL-008).

Abbreviations

Ac = acetyl

rt = room temperature

DEAD = diethyl azodicarboxylate

THF = tetrahydrofuran

DCM = dichloromethane

TFA = trifluoroacetic acid

HOSu = *N*-hydroxysuccinimide

EDCI = *N*-(3-dimethylaminopropyl)-*N*'-ethylcarbodiimide hydrochloride

DIC = *N*, *N*'-diisopropylcarbodiimide

DMF = *N*, *N*-dimethylforamide

$DppoNH_2$ = *O*-(diphenylphosphoryl)hydroxylamine

References

[1] A.J. Wolf, D. M. Underhill, Peptidoglycan recognition by the innate immune system, Nat. Rev. Immunol. 18 (2018) 243−254.

[2] R.G. Correa, S. Milutinovic, J.C. Reed, Roles of NOD1 (NLRC1) and NOD2 (NLRC2) in innate immunity and inflammatory diseases, Biosci. Rep. 32 (2012) 597–608

[3] J.H. Richard, R.L. Ferrero, D.J. Philpott, S.E. Girardin, Nod-like proteins in immunity, inflammation and disease, Nat. Immunol. 7 (2006) 1250−1257.

[4] N. Inohara, G. Nuñez, NODs: intracellular proteins involved in inflammation and apoptosis, Nat. Rev. Immunol. 3 (2003) 371−382.

[5] Ž. Jakopin, Nucleotide-binding oligomerization domain (NOD) inhibitors: A

rational approach toward inhibition of NOD signaling pathway, J. Med. Chem. 57 (2014) 6897−6918.

[6] T. Mukherjee, E.S. Hovingh, E.G. Foerster, M. Abdel-Nour, D.J. Philpott, S.E. Girardin, NOD1 and NOD2 in inflammation, immunity and disease, Arch Biochem Biophys. 670 (2019) 69−81.

[7] A. Biswas, Y.-J. Liu, L. Hao, A. Mizoguchi, N.H. Salzman, C.L. Bevins, K.S. Kobayashi, Induction and rescue of nod2-dependent Th1-driven granulomatous inflammation of the ileum, Proc. Natl. Acad. Sci. U. S. A. 107 (2010) 14739−14744.

[8] J. Jamontt, S. Petit, N. Clark, S.J. Parkinson, P. Smith, Nucleotide-binding oligomerization domain 2 signaling promotes hyperresponsive macrophages and colitis in IL-10-deficient mice, J. Immunol. 190 (2013) 2948−2958.

[9] K.P. Foley, B. Desai, A. Vossenkämper, M.A. Reilly, P. Biancheri, L. Wang, D.B. Lipshutz, J. Connor, M. Miller, P.A. Haile, L.N. Casillas, B.J. Votta, P.J. Gough, T.T. MacDonald, C.H. Wouters, C.D. Rose, J. Bertin, OR3−001−RIP2 kinase is activated in blau syndrome and IBD, Pediatr. Rheumatol. 11 (2013) (Suppl 1): A3.

[10] P. Sfriso, F. Caso, S. Tognon, P. Galozzi, A. Gava, L. Punzi, Blau syndrome, clinical and genetic aspects, Autoimmun. Rev. 12 (2012) 44−51.

[11] C. Ospelt, F. Brentano, A. Jüngel, Y. Rengel, C. Kolling, B.A. Michel, R.E. Gay, S. Gay, Expression, regulation, and signaling of the pattern-recognition receptor nucleotide-binding oligomerization domain 2 in rheumatoid arthritis synovial fibroblasts, Arthritis Rheum. 60 (2009) 355−363.

[12] H.L. Rosenzweig, M.J. Jann, E.E. Vance, S.R. Planck, J.T. Rosenbaum, M.P.

Davey, Nucleotide-binding oligomerization domain 2 and Toll-like receptor 2 function independently in a murine model of arthritis triggered by intraarticular peptidoglycan, Arthritis Rheum. 62 (2010) 1051−1059.

[13] M. Wikén, J. Grunewald, A. Eklund, J. Wahlström, Higher monocyte expression of TLR2 and TLR4, and enhanced proinflammatory synergy of TLR2 with NOD2 stimulation in sarcoidosis, J. Clin. Immunol. 29 (2009) 78−89.

[14] S.L. Rivers, A. Klip, A. Giacca, NOD1: An interface between innate immunity and insulin resistance, Endocrinology 160 (2019) 1021−1030.

[15] P. Hysi, M. Kabesch, M.F. Moffatt, M. Schedel, D. Carr, Y. Zhang, B. Boardman, E. von Mutius, S.K. Weiland, W. Leupold, C. Fritzsch, N. Klopp, A.W. Musk, A. James, G. Nunez, N. Inohara, W.O.C. Cookson, NOD1 variation, immunoglobulin E and asthma, Hum. Mol. Genet. 14 (2005) 935−941.

[16] F.Y. Goh, K.L.T.P. Cook, N. Upton, L. Tao, L.C. Lah, B.P. Leung, W.S.F. Wong, Receptor-interacting protein 2 gene silencing attenuates allergic airway inflammation, J. Immunol. 191 (2013) 2691−2699.

[17] J.C. Jun, F. Cominelli, D.W. Abbott, RIP2 activity in inflammatory disease and implications for novel therapeutics, J. Leukocyte Biol. 94 (2013) 927−932.

[18] S. Nabergoj, I. Mlinarič-Raščan, Ž. Jakopin, Harnessing the untapped potential of nucleotide-binding oligomerization domain ligands for cancer immunotherapy, Med Res Rev. 39 (2019) 1447–1484.

[19] F.J. Velloso, M. Trombetta-Lima, V. Anschau, M.C. Sogayar, R.G. Correa, NOD-like receptors: major players (and targets) in the interface between innate

immunity and cancer, Bioscience Rep. 39 (2019) BSR20181709.

[20] R. Daillère, M. Vétizou, N. Waldschmitt, T. Yamazaki, C. Isnard, V. Poirier-Colame, C.P.M. Duong, C. Flament, P. Lepage, M.P. Roberti, B. Routy, N. Jacquelot, L. Apetoh, S. Becharef, S. Rusakiewicz, P. Langella, H. Sokol, G. Kroemer, D. Enot, A. Roux, A. Eggermont, E. Tartour, L. Johannes, P.-L. Woerther, E. Chachaty, J.-C. Soria, E. Golden, S. Formenti, M. Plebanski, M. Madondo, P. Rosenstiel, D. Raoult, V. Cattoir, I.G. Boneca, M. Chamaillard, L. Zitvogel. Enterococcus hirae and barnesiella intestinihominis facilitate cyclophosphamide-induced therapeutic immunomodulatory effects, Immunity, 45 (2016) 931−943.

[21] H.Y. Jiang, S. Najmeh, G. Martel, E. MacFadden-Murphy, R. Farias, P. Savage, A. Leone, L. Roussel, J. Cools-Lartigue, S. Gowing, J. Berube, B. Giannias, F. Bourdeau, C.H.F. Chan, J.D. Spicer, R. McClure, M. Park, S. Rousseau, L. E. Ferri, Activation of the pattern recognition receptor NOD1 augments colon cancer metastasis, Protein Cell 11 (2020) 187−201.

[22] G. Magnuson, P. Khan, H. Yuan, B. Brown, D.B. Divlianska, D. Stonich, S. Peddibhotla, Y. Su, S. Dad, E. Sergienko, T.D.Y. Chung, G.P. Roth, C. Wimer, P. Diaz, R.G. Correa, J.C. Reed, High Throughput screening assays for NOD1 inhibitors-Probe 2. Probe Reports from the NIH Molecular Libraries Program, 2010. Bethesda (MD).

[23] G. Magnuson, P. Khan, H. Yuan, B. Brown, D.B. Divlianska, D. Stonich, S. Peddibhotla, Y. Su, S. Dad, E. Sergienko, T.D.Y. Chung, G.P. Roth, C. Wimer, P. Diaz, R.G. Correa, J.C. Reed, High Throughput screening assays for NOD1

inhibitors-Probe 1. Probe Reports from the NIH Molecular Libraries Program, 2010. Bethesda (MD).

[24] P.M. Khan, R.G. Correa, D.B. Divlianska, S. Peddibhotla, E.H. Sessions, G. Magnuson, B. Brown, E. Suyama, H. Yuan, A. Mangravita-Novo, M. Vicchiarelli, Y. Su, S. Vasile, L.H. Smith, P.W. Diaz, J.C. Reed, G.P. Roth, Identification of inhibitors of NOD1-induced nuclear factor-κB activation, ACS Med. Chem. Lett. 2 (2011) 780−785.

[25] D.J. Rickard, C.A. Sehon, V. Kasparcova, L.A. Kallal, X. Zeng, M.N. Montoute, T. Chordia, D.D. Poore, H. Li, Z. Wu, P.M. Eidam, P.A. Haile, J. Yu, J.G. Emery, R.W. Marquis, P.J. Gough, J. Bertin, Identification of benzimidazole diamides as selective inhibitors of the nucleotide-binding oligomerization domain 2 (NOD2) signaling pathway, PloS One 8 (2013), e69619.

[26] S. Guzelj, M. Gobec, D. Urbančič, I. Mlinarič-Raščan a, E. Corsini, Ž Jakopin, Structural features and functional activities of benzimidazoles as NOD2 antagonists, Eur. J. Med. Chem. 190 (2020) 112089.

[27] K. Keček Plešec, D. Urbančič, M. Gobec, A. Pekošak, T. Tomašič, M. Anderluh, I. Mlinarič-Raščan, Ž. Jakopin, Identification of indole scaffoldbased dual inhibitors of NOD1 and NOD2, Bioorg. Med. Chem. 24 (2016) 5221−5234.

[28] Y. Dong, S. Wang, C. Wang, Z. Li, Y. Ma, and G. Liu, Antagonizing NOD2 signaling with conjugates of paclitaxel and muramyl dipeptide derivatives sensitizes paclitaxel therapy and significantly prevents tumor metastasis, J. Med. Chem. 60 (2017) 1219−1224.

[29] X. Wen, P. Zheng, Y. Ma, Y. Ou, W. Huang, S. Li, S. Liu, X. Zhang, Z. Wang, Q. Zhang, W. Cheng, R. Lin, H. Li, Y. Cai, C. Hu, N. Wu, L. Wan, T. Pan, J. Rao, X. Bei, W. Wu, J. Jin, J. Yan, G. Liu, Salutaxel, a conjugate of docetaxel and a muramyl dipeptide (MDP) analogue, acts as multifunctional prodrug that inhibits tumor growth and metastasis, J. Med. Chem. 61 (2018) 1519−1540.

[30] S. Wang, J. Yang, X. Li, Z. Liu, Y. Wu, G. Si, Y. Tao, N. Zhao, X. Hu, Y. Ma, G. Liu, Discovery of 1,4-benzodiazepine-2,5-dione (BZD) derivatives as dual nucleotide binding oligomerization domain containing 1/2(NOD1/NOD2) antagonists sensitizing paclitaxel (PTX) to suppress lewis lung carcinoma (LLC) growth *in vivo*, J. Med. Chem. 60 (2017) 5162−5192.

[31] X. Li, Y. Dong, F. Qu, G. Liu, Synthesis of benzofused five-ring sultams via Rh-catalyzed C−H olefination directed by an *N*-Ac-substituted sulfonamide group, J. Org. Chem. 80 (2015) 790−798.

[32] Ž. Jakopin, E. Corsini, THP-1 cells and pro-inflammatory cytokine production: an in vitro tool for functional characterization of NOD1/NOD2 antagonists, Int. J. Mol. Sci. 20 (2019) 4265.

[33] R. Caruso, N. Warner, N. Inohara, G. Núñez, NOD1 and NOD2: signaling, host defense, and inflammatory disease, Immunity, 41 (2014) 898−908.

Hightlights

- A new class of derivatives of dual NOD1/NOD2 antagonists with novel benzofused five-membered sultams was designed and synthesized.
- The most promising compound 14k exhibited promising potent inhibitory activity against NOD1 and NOD2 with IC_{50} values of 1.05 and 0.93 μM, respectively.
- Compound 14k had moderate inhibition effect on cytokine production in response to stimulation with MDP *in vivo.*

清華大學 药学院
SCHOOL OF PHARMACEUTICAL SCIENCES
TSINGHUA UNIVERSITY

European Journal of Medicinal Chemistry
2020/2/21

Dear Editors,

The authors declare that they have no known competing financial interests or personal relationships that could have appeared to influence the work reported in this paper.

Sincerely yours

Gang LIU, Ph.D., Professor of Medicinal Chemistry
Tsinghua University
School of Pharmaceutical Sciences
Renhuan Building, Rm 311
Beijing, CHINA
Zip:100084
Tel: 086-10-62797740
Email:gangliu27@tsinghua.edu.cn
http://www.sps.tsinghua.edu.cn/